Issues in Predictability

H. Abarbanel
S. Koonin
H. Levine
G. MacDonald
O. Rothaus

December 1991

JSR-90-320

JASON
The MITRE Corporation
7525 Colshire Drive
McLean, Virginia 22102-3481
(703) 883-6997

REPORT DOCUMENTATION PAGE

Form Approved
OMB No. 0704-0188

1. AGENCY USE ONLY (Leave blank)	2. REPORT DATE	3. REPORT TYPE AND DATES COVERED
	December 30, 1991	

4. TITLE AND SUBTITLE

Issues In Predictability

5. FUNDING NUMBERS

PR - 8503Z

6. AUTHOR(S)

H. Abarbanel, S. Koonin, H. Levine, G. MacDonald,
O. Rothaus

7. PERFORMING ORGANIZATION NAME(S) AND ADDRESS(ES)

The MITRE Corporation
JASON Program Office A10
7525 Colshire Drive
McLean, VA 22102

8. PERFORMING ORGANIZATION REPORT NUMBER

JSR-90-320

9. SPONSORING/MONITORING AGENCY NAME(S) AND ADDRESS(ES)

Department of Energy
Washington, DC 20585

10. SPONSORING/MONITORING AGENCY REPORT NUMBER

JSR-90-320

11. SUPPLEMENTARY NOTES

12a. DISTRIBUTION/AVAILABILITY STATEMENT

12b. DISTRIBUTION CODE

13. ABSTRACT *(Maximum 200 words)*

Since the beginning of the greenhouse debate, policy makers have demanded from the scientific community predictions of future climate in limited geographical areas and limited time intervals. Current climate models clearly do not have such capabilities, as is demonstrated by large disagreements among the models of continental size regions. Largely lost in the debate are fundamental questions such as: What is meant by predictability? What can be predicted and over what time and length scale? What errors can be expected from predictions? This report explores some of the issues by analyzing toy models of climate and existing data sets of global annual average surface air temperature.

14. SUBJECT TERMS

climate, Lorenz, climate forecasting, Hansen-Lebedeff, low-frequency

15. NUMBER OF PAGES

16. PRICE CODE

17. SECURITY CLASSIFICATION OF REPORT	18. SECURITY CLASSIFICATION OF THIS PAGE	19. SECURITY CLASSIFICATION OF ABSTRACT	20. LIMITATION OF ABSTRACT
UNCLASSIFIED	UNCLASSIFIED	UNCLASSIFIED	SAR

Contents

1 INTRODUCTION

Since the beginning of the greenhouse debate, policy makers have demanded from the scientific community predictions of future climate in limited geographical areas (e.g., Congressional Districts) and limited time intervals (e.g., Convention Time, 2000). Current climate models clearly do not have such capabilities, as is demonstrated by large disagreements among the models of continental size regions. Government and private groups have proposed programs such as DOE's CHAMMP and UCAR's CSMP to remedy the situation. Largely lost in the debate are fundamental questions such as: What is meant by predictability? What can be predicted and over what time and length scale? What errors can be expected from predictions? This report explores some of the issues by analyzing toy models of climate and existing data sets of global annual average surface air temperature.

We first point out in Section 2 why there is a problem. In these considerations we have been much influenced by the work of Lorenz (1963, 1969, 1976, 1984a, b), who in a long series of papers has thoroughly raised the issue of atmospheric predictability. In Section 3 we describe our understanding of why the current modeling community is so optimistic about fine-scale, long-term climate predictions. We raise some questions with respect to this point of view in Section 4. Section 5 describes one approach to the problem of prediction: That approach based on reducing the dimension of a high-dimensional attractor by averaging. We describe the results of analysis of time series derived from model runs and data sets in Section 6. Our summary views are presented in Section 7.

While this report raises the issue of predictability, we do not wish to

question in any way the value of attempts to model climate. Since real-world climate experiments, other than the one currently underway on the greenhouse, cannot be conducted, an understanding of climate can only be achieved through computer models. Our basic concern is that models will be used to arrive at predictions which may or may not be meaningful, rather than be used to deepen our understanding of climate processes. This deeper understanding of climate may lead to alternative, more reliable methods of forecasting than the use of GCMs. At the very least, a more complete understanding of climate dynamics must lead to much improved future GCMs.

2 WHAT IS THE PROBLEM?

The climate of a region is often thought of as the weather which ordinarily occurs there. In more scientific terms, climate may be defined with a set of long-term statistical properties. Following the work of Lorenz, there is widespread consensus that weather is chaotic, with a loss of coherence (for consensus neighboring initial conditions) in one to two weeks. This observation places limits on the long-term predictability of weather. Since climate is defined in terms of averages, the question of predictability is: "Do there exist length and time scales such that the evolution of averaged variables (temperature, precipitation, etc.) on these scales is <u>not</u> extremely sensitive to initial conditions?" This statement can be quantified in the following way: Given the initial conditions, specified with some small error, the system will be predictable if there is a time scale τ and a length scale L such that at some later time t, the averaged variables

$$\bar{T}(x,t) = \frac{1}{L\tau} \int_{t-\frac{\tau}{2}}^{t+\frac{\tau}{2}} dt' \int_{x-\frac{L}{2}}^{x+\frac{L}{2}} T(x',t')dx' \qquad (2-1)$$

satisfy dynamics which do not have exponential growth of small errors.

Equation (2-1) explicitly introduces the averaging time τ and the averaging length L. In discussions of predictability, both quantities should be considered. Even if there is a time scale τ over which the global average temperature, for example, is predictable, we can anticipate there will be some length scale $L(\tau)$, less than global, for which predictability fails at the same averaging time.

While climate is conventionally defined by averages, situations may arise where it is of interest to predict quantities other than averages. Examples of

alternative quantities include the maximum intensity reached by storms in a given period or the minimum rainfall. The problem of predicting extreme events is treated in Abarbanel et al. (1990).

Nonlinear dynamics provides a framework in which to discuss the meaning of predictability. We assume that the system under investigation can be described by a set of first order ordinary differential equations

$$\dot{y}_i(t) = f_i(y_j, t) \quad i, j = 1, \cdots n$$

where $y_i(t)$ are selected state variables and n is finite. The orbit of the dynamical system, as determined by the evolution of the state variables y and perturbed by small random variations (round-off errors due to floating point truncations in computer models, or the "external" noise in observational systems), is asymptotically concentrated on an attractor of finite dimension, and there exists an invariant asymptotic measure ρ that is stable under the perturbations. The probability measure ρ describes how frequently various parts of the attractor are visited by an orbit. A picture of the physical measure can be obtained by plotting a histogram of the value of the variable y. What is the predictability of the vector y?

Given a small ball around any initial condition $y(0)$, the evolution of this ball in time may be used to formalize what we mean by predictability of the system in a physical sense if not in a precise mathematical way.

In particular, if we assume that the solution of the set of ordinary differential equations lies within a closed and bounded region, R, of n-space, the rate at which this ball disperses throughout the region R is one measure of its predictability. If the geometry of the ball is unchanged, the rate of dispersion vanishes and the system is perfectly predictable. If the set of

equations is linear, the functions f are well behaved in some sense, and there is no additive noise, then the rate of dispersion is zero and the system is predictable.

When there is a meaningful invariant measure on R, it may be used to describe the rate of dispersion. Ergodic theory provides an extensive basis for such analysis.

Abarbanel et al. (1990) show that a toy model of climate, the Lorenz 27-variable model, generates values of the surface air temperature that are indistinguishable from normally distributed random variates both about the mean and even in the tails of the distribution after integration of several thousand model years at 6-hour time steps. Long surface air temperature records (up to 318 years) show similar properties once a linear trend has been removed. The values of temperature are indistinguishable from normally distributed random variables both about the mean and for extreme values.

These results could suggest that the deterministic system generated by the Lorenz 27-variable model is closely correlated to a function of a Bernoulli shift. This might indicate that the Lorenz 27-variable model may be factored into simple components, one of which is a function of the Bernoulli shift. The Lorenz 27-variable model data also has a finite dimension, so it is distinguishable from "noise."

In terms of predictability, these observations indicate that the rate of dispersion of a ball for the model system and for the observed data is at an extreme where every disk undergoes a uniform and complete dispersion at a known rate, the entropy. If climate, in the absence of external forcing, approximates some complex function of a Bernoulli shift, then the prospects

for long-term prediction are dim. Obviously these questions need serious study.

The physical dimensions of the region R in n-space are roughly determined by the conservation equations associated with the system of equations for y (Abarbanel et al. 1990). For a system based on a function of a Bernoulli shift, the dispersion in time of the initial ball will proceed out to the boundaries of R. The extreme values reached by the variables y are bounded by the boundaries of R. In a "true" random variable that is normally distributed, the extremes are unbounded, growing as $(\log k)^{\frac{1}{2}}$ where k is the number of time steps. Both in the extreme values and in the manner in which the region R is populated, a physical system will differ from a "truly random" process. This is the case even when the physical dynamics is driven by an embedded Bernoulli shift. In practical random number generators, deviations from true randomness are set by recurrence times due to the finite state size of the $y_i(t)$.

Finally we note that the Bernoulli shift involves stretching and back folding of the unit internal under the action of $\sigma(y)$. This mapping is closely related to another example, the Smale horseshoe, which is a hyperbolic limit set that has been a principal motivating force in the development of modern dynamical systems. A horseshoe arises whenever the system has transverse homoclinic orbits. These close analogues may be of use in untangling the underlying dynamical complexities of the Lorenz 27-variable system.

3 CONVENTIONAL VIEWS WITH RESPECT TO CLIMATE FORECASTING

A commonly held view within the modeling community is that there is a sharp distinction between the fast elements of the atmosphere-ocean system and the slow elements (Hasselmann, 1976). The slow elements, ocean circulations, are altered by the fast components, atmospheric weather systems, which in turn are altered by the slow components. These interactions give rise to a variance that is sometimes described as natural variability. Optimistic predictors acknowledge that the fast components are chaotic but claim the slow components are not, despite the interactions between fast and slow. Just as a matter of principle, this cannot be true in a coupled system.

The supporters of predictability recognize that the larger horizontal scales of the atmosphere require that the atmosphere as a whole be treated as chaotic. The eddies and gyres in the ocean have a much smaller spatial scale (100 km) than weather systems in the atmosphere. While the gyres and associated structure are chaotic, the large-scale features of ocean circulation are considered to be non-chaotic and predictable. The predictability of this slow component of the ocean leads to the conclusion that the climate system as a whole is predictable. Certain features of atmospheric climate show cyclical behavior, again suggesting predictability. These include the seasonal fluctuations of temperature over continental size areas, the seasonal development of the monsoons, etc.

These observations lead to the common assumption used in climate prediction that the ocean-atmosphere system is in balance with the forcing.

Variations in insolation give rise to a seasonal forcing leading to the continental seasons and the monsoons. The slow orbital variations in insolation of the past lead to a smooth atmospheric response and to the ice ages. The slow ocean motions are similarly taken as an external forcing that leads to smooth and thus predictable changes in climate. As long as the forcing changes slowly, the mean state of the climate system is stable, and if there is a change in forcing, the mean state will change until it is in balance with the forcing. In particular, as the composition of the atmosphere changes as a result of society activities, the radiative forcing changes slowly and the mean state of the atmosphere responds. On the basis of these considerations, many in the modeling community believe that long-term, fine- grained resolution predictability can be achieved.

4 A SKEPTICAL VIEW OF CLIMATE FORECASTING

The real issue of predictability is whether the atmosphere-ocean systems constitutes a chaotic dynamical system at all time scales, whatever spatial filtering may be applied. The conventional view holds that it is chaotic in the fast atmospheric motions, but that the slow elements of ocean circulation are not. Chaotic dynamical systems can develop very long-term aperiodic fluctuations with time scales much longer than any of the obvious time constants which appear in the governing laws. In fact, periods of virtually any length could occur even if the atmosphere-ocean system experiences no change in the external forcing. While the effect of a change in external forcing may be predictable, this change will be superposed on the internal fluctuations. The externally forced changes may be predictable, while the internal fluctuations are not.

In this context it is important to distinguish external forcing from "internal" forcing. Changes in solar constant are external, but changes in long-term ocean circulation are internal to the atmosphere-ocean system and cannot be assumed to be independent from the rest of the system. This interconnection follows directly from the nonlinear nature of the governing equations.

In a related report (Abarbanel et al., 1990), we present an analysis of a long (134 years) global annual average surface air temperature record, which indicates chaotic behavior at all time scales represented in the record. If a linear trend, possibly due to greenhouse forcing, is removed from the record, the residuals show a normal distribution both about the mean and in the tails of the distribution. The fact that the extremes are consistent with the

assumption that the statistical distribution is normal suggest that even at low frequencies the behavior is chaotic. The power spectrum strongly peaks at the low frequencies. The high-amplitude, low-frequency variations carry the shorter period fluctuations up and down and thus go far toward determining the range – the difference between maximum and minimum temperature – of the distribution. Similarly, the Lorenz 27-variable model of climate (Abarbanel et al., 1990) shows chaotic behavior at low frequencies with both extreme values and those near the mean exhibiting behavior indistinguishable from that of a sample drawn from a normal population (see Section 2).

While the above arguments do not prove that the atmosphere-ocean system is chaotic at all time scales, they do strongly imply that the issue needs further investigation. Extremely long (1000 years or more) runs of coupled atmosphere-ocean models are required to study the issue of whether the system exhibits chaotic behavior at all time scales of interest to considerations of climate. Similarly long runs of the atmosphere alone are needed to determine the time scales over which uncoupled atmospheric motion is chaotic. For example, the Lorenz 27-variable model shows long-period internal fluctuations associated with long-term variations in albedo due to shifts in average cloud cover even though there is no ocean circulation in the model.

5 REDUCING THE DIMENSION OF THE ATTRACTOR BY AVERAGING

The criteria for predictability given in (2-1) can be translated into a statement about the correlation function on some type of dynamical attractor for the system. If we consider only the effects of time averaging, the variance of $\bar{T}$ (see Equation (2-1)) is

$$\text{var}\,[\bar{T}] = \frac{1}{\tau^2}\int\int \left(E[T(t')T(t'')] - E[t']\,E[t'']\right)\,dt'\,dt''. \qquad (5-1)$$

If the process is taken to be stationary (a strong assumption) and ergodic, the ensemble average (denoted by E) can be replaced by time average, yielding

$$\text{var}\,[\hat{T}] = \frac{1}{\tau^2}\int\int dt'dt'' \int e^{i\omega(t'-t'')}\,S(\omega)\,d\omega \qquad (5-2)$$

where $S(\omega)$ is the spectral density of the field T. This yields

$$\text{var}\,[\hat{T}] = \int \left(\frac{\sin\,(\omega\,\tau)}{\omega\,\tau}\right)^2 S(\omega)\,d\omega, \qquad (5-3)$$

where the first factor in the integral acts as a low-pass filter, weighting all parts of the spectrum below τ^{-1}. Equation (5-3) implies that predictability, free from chaos, requires that the averaging in time, determined by τ, be sufficiently long that no significant power remains after the filtering.

From Equation (5-3) we note the importance of the low-frequency components in determining predictability. If these components are chaotic, then long-term prediction is impossible although short-term prediction using the methods of nonlinear dynamics may be feasible (Abarbanel, 1990). Climate records, as well as most geophysical records, show strong red noise. Figure 1 shows a reconstruction of the global annual average surface temperature derived from observations at land stations (Hansen and Lebedeff, 1987, 1988).

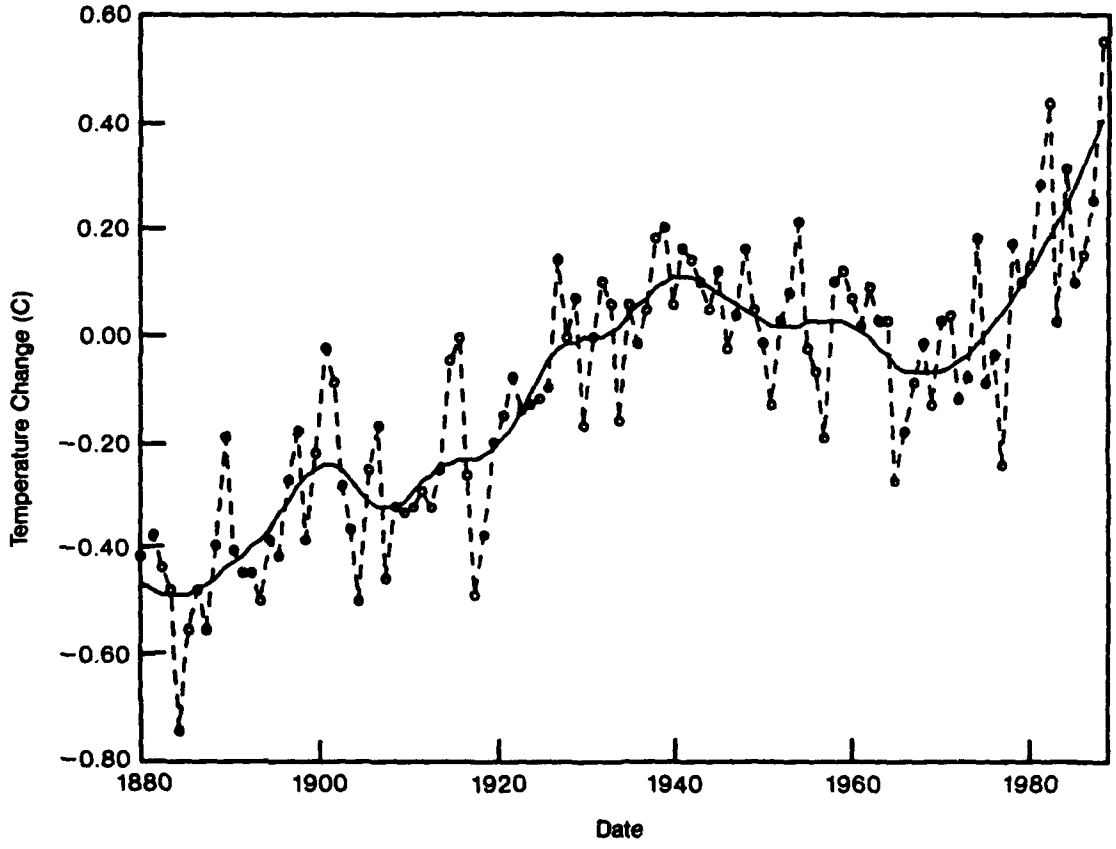

Figure 1. Variation of global annual average surface air temperature (Hansen and Lebedeff, 1987, 1988). The solid curve is a five-year moving average.

The power spectrum (normalized to unit variance) is shown in Figure 2. The power drops rapidly from zero frequency to a first minimum at 0.04 cpyr. A second global annual average surface air temperature record is shown in Figure 3 (Jones 1988, and personal communication, 1990). The data for Figure 3 include observations made at sea by vessels as well as land-based observations. The power spectrum for the record given in Figure 3 is shown in Figure 4. Again there is a peak at zero frequency but the drop-off at higher frequencies is not quite as sharp as that shown in Figure 2.

The irregularity of the temporal curves and the red noise characteristic of the power spectrum exhibited by data records show clearly in simple models of the atmosphere. Lorenz (1984b) has developed a low-order model in 27 variables. The physical variables include the mixing ratios of water vapor and liquid water as well as the air surface temperature, ocean surface temperature, pressure and the usual dynamical variables. In Lorenz's model, the ocean and atmosphere exchange heat and water through evaporation and precipitation. The model also produces clouds, which reflect incoming solar radiation, while both phases of water absorb and re-emit infrared radiation. Figure 5 shows a series of snapshots of surface air temperature at one-year intervals for 1000-years. The power spectrum for the 1000 year Lorenz record is shown in Figure 6. The first minimum in the spectrum is at 0.04 cpyr but the spectrum continues to drop to 0.1 cpyr before entering the flatter spectral region.

The strong low-frequency peaks exhibited by data sets and model runs imply from (5-3) that the variance for $\bar{T}$ will be large. Since there is energy in the records up to the length of the record we cannot use averages to totally eliminate chaotic noise if the low-frequency peaks represent chaos. Sections 2 and 4 describe one line of evidence, statistics of extremes, that suggests that

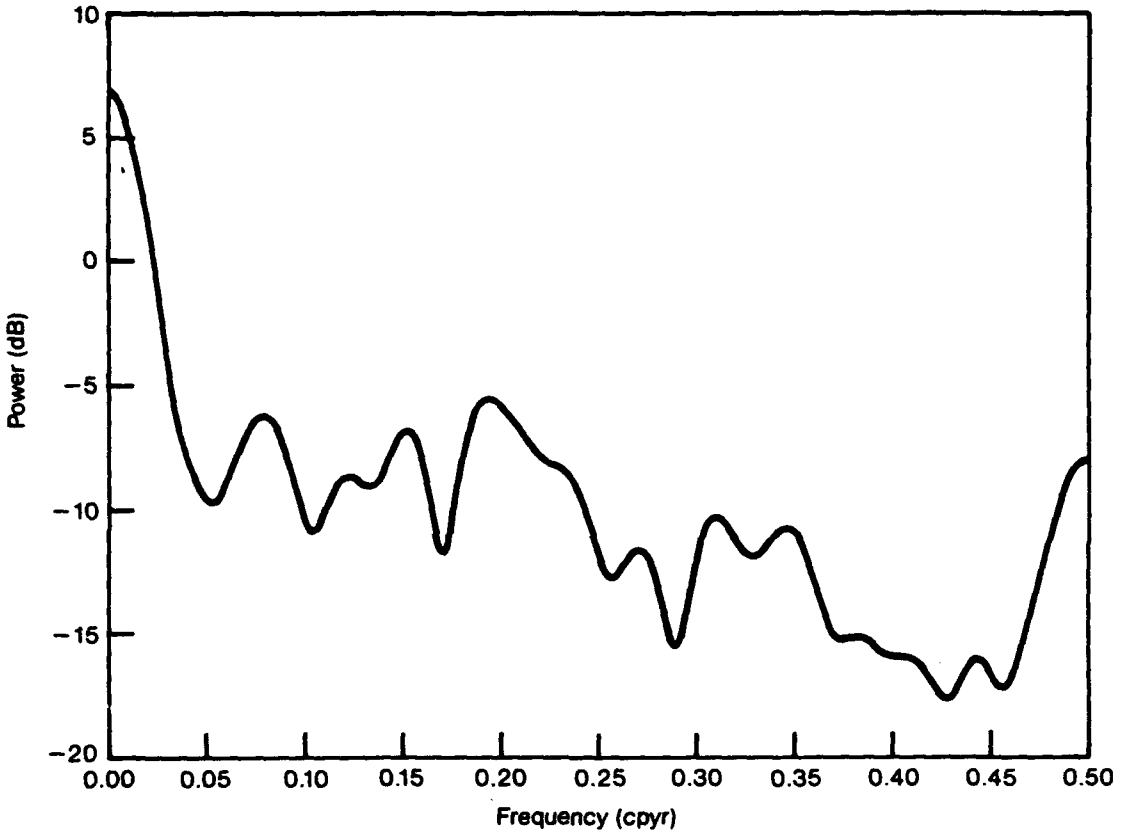

Figure 2. The power spectrum for the global annual average surface air temperature record shown in Figure 1. The data have been normalized to zero mean and unit variance.

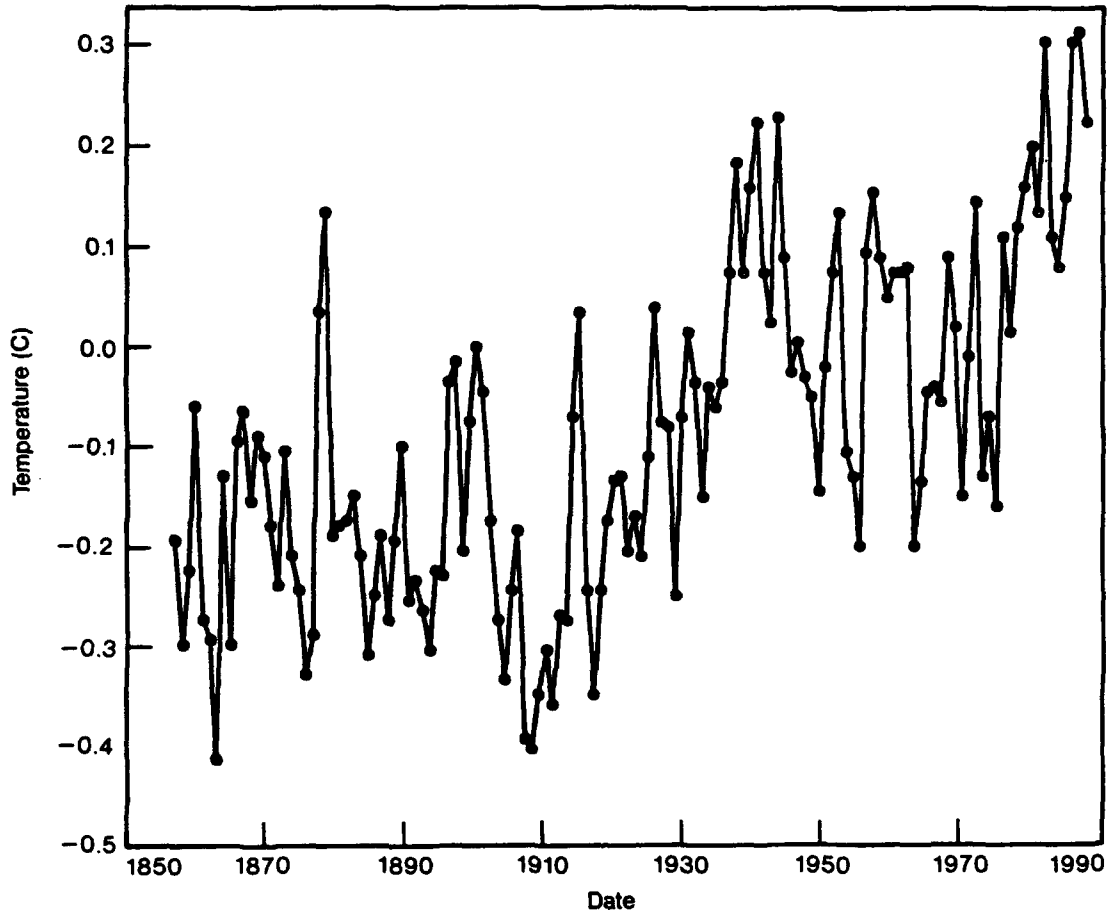

Figure 3. Record of global annual average surface air temperature (Jones, 1988, and personal communication, 1990).

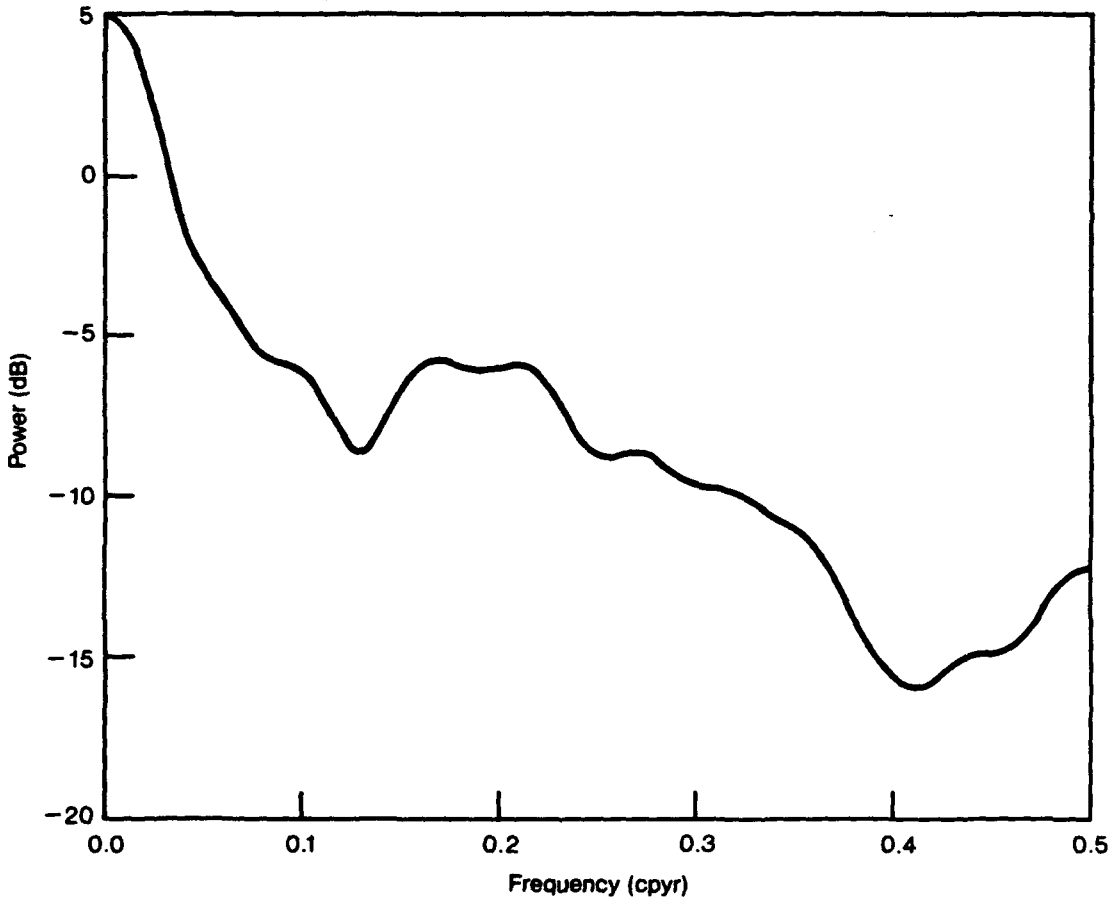

Figure 4. Power spectrum for record of global annual average surface air temperature record shown in Figure 3. The data have been normalized to zero mean and unit variance.

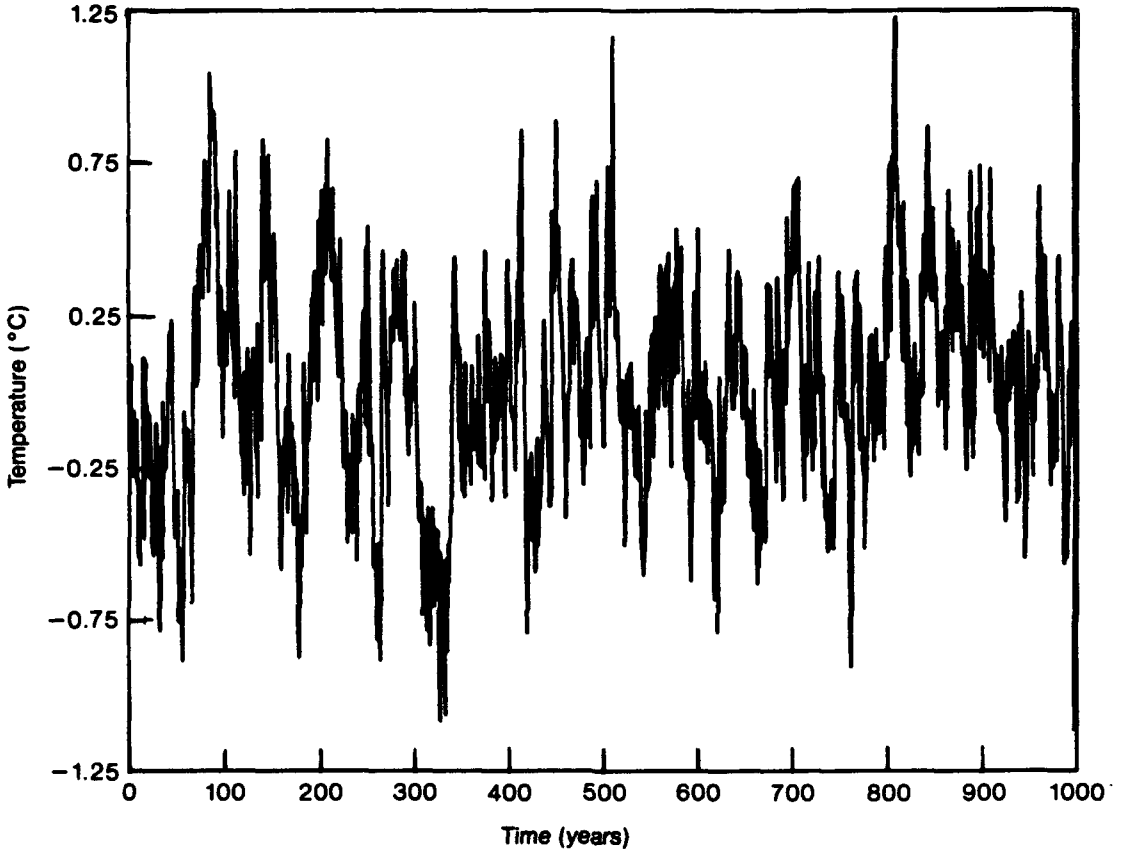

Figure 5. Variations of the sea-level air temperature for 1,000 years in a numerical solution to Lorenz's 27-variable model of the atmosphere (Lorenz, 1984b).

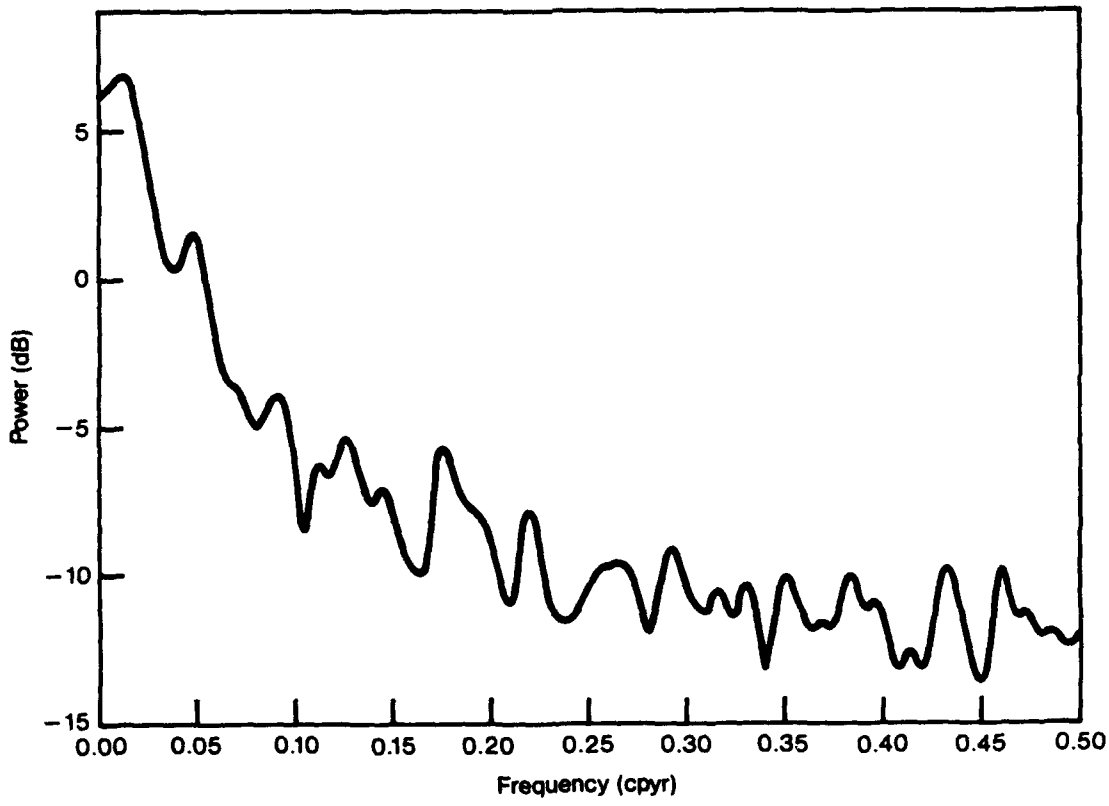

Figure 6. Power spectrum for the 1,000-year temperature record shown in Figure 5.

the low-frequency region is chaotic. If we cannot obtain long enough time averages to eliminate chaos, we might be able to average over long enough time to reduce the dimension of the attractor governing the dynamic system. As noted above, there are emerging techniques for short-range predictions based on the fact that low-dimensional systems can be reconstructed and integrated forward in time deterministically. This procedure would allow prediction up to a time characaterized by the inverse of the largest Lyapunov exponent. While prediction in the long term may not be possible, prediction in the short term may be.

In order to test the hypothesis that averaging reduces the dimension of the attractor we use a record generated by the Lorenz 27-variable model (see Figures 5 and 6). Ten thousands years of monthly averaged surface air temperature were used to obtain the correlation dimensions of the attractor. The dimension for the original record without filtering is 6.8. The record was then low-pass filtered at 0.08, 0.06, 0.04 and 0.02 cpyr, corresponding to longer and longer averaging times. The results are displayed in Figure 7. The dimension drops approximately linearly with the filter cutoff frequency, reaching a value of 3.35 for a record containing energy below 0.02 cpyr. The short length of the observed data records we have examined makes it impossible to estimate either the dimensions of either the original data sets or filtered versions of these data sets.

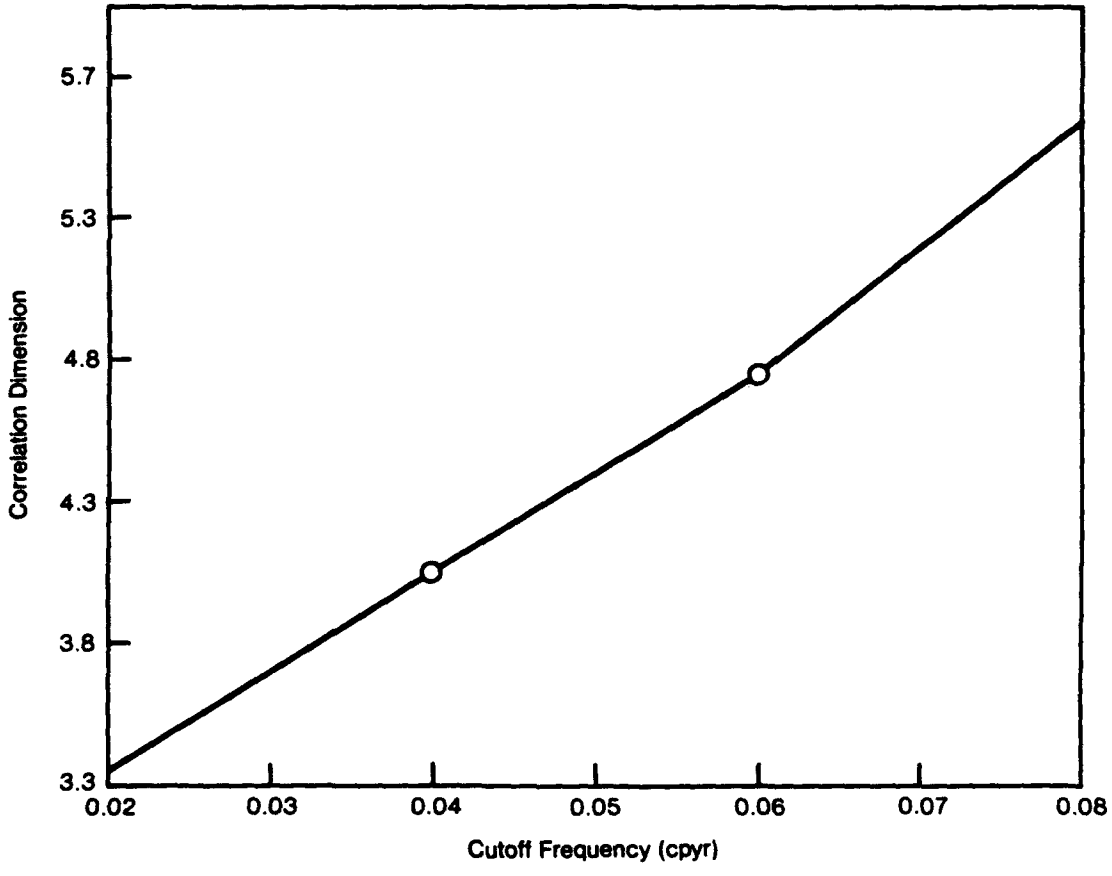

Figure 7. Variation of the correlation dimension from the Lorenz 27-variable model surface air temperature with the cutoff frequency of a low-pass filter. The record consists of 10,000 years of monthly averaged surface air temperatures. The dimension of the unfiltered record is 6.8.

6 EXAMPLES OF FILTERED SERIES

6.1 Introduction

In order to facilitate comparison among series, we have used a uniform cutoff frequency of 0.04 cpyr. If the data sets contain a linear trend, the trend as determined by a least squares fit is first removed from the record. This means that the low-frequency content of the record has been broken into two parts: the linear trend and the low-frequency part of the residual.

We first discuss data sets in Section 6.2 and then model results in Section 6.3. After summarizing the analysis in Section 6.4, an alternate form representing the results is described in Section 6.5. The alternate representation is one of approximate phase plots in which the average rate of change of temperature is plotted against the average temperature.

6.2 Data Sets

The low-frequency components of the Hansen-Lebedeff temperature record (see Figure 1) are given in Figure 8. The residual "noise" obtained after removal of the low- frequency components and a linear trend is shown in Figure 9. The peak to peak variability in the smoothed curve (Figure 8) is about 0.35° compared with about 0.4° peak to peak in the residuals. Clearly the low-frequency wave can carry the higher-frequency components up and down to give a high total peak to peak variation in the unfiltered record.

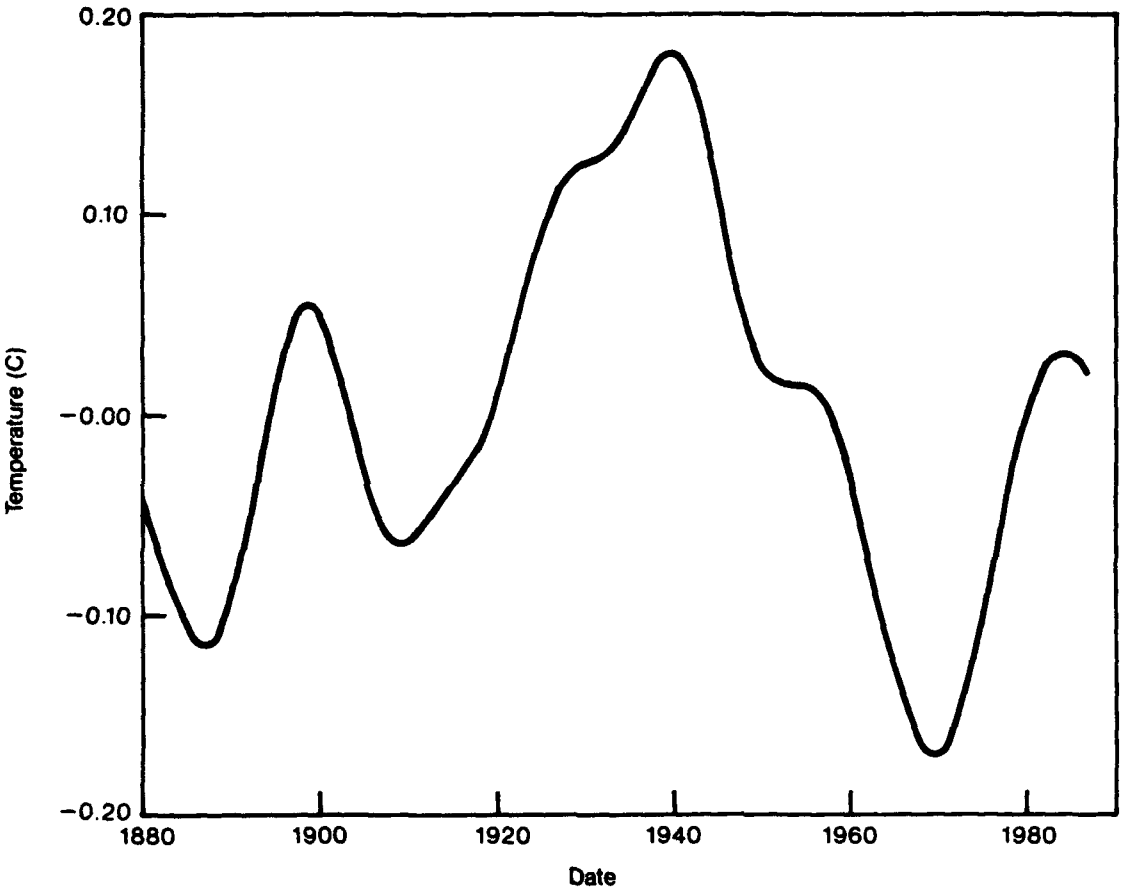

Figure 8. The low-frequency components (< 0.04 cpyr) of the global annual average surface air temperature from Hansen and Lebedeff (see Figure 1).

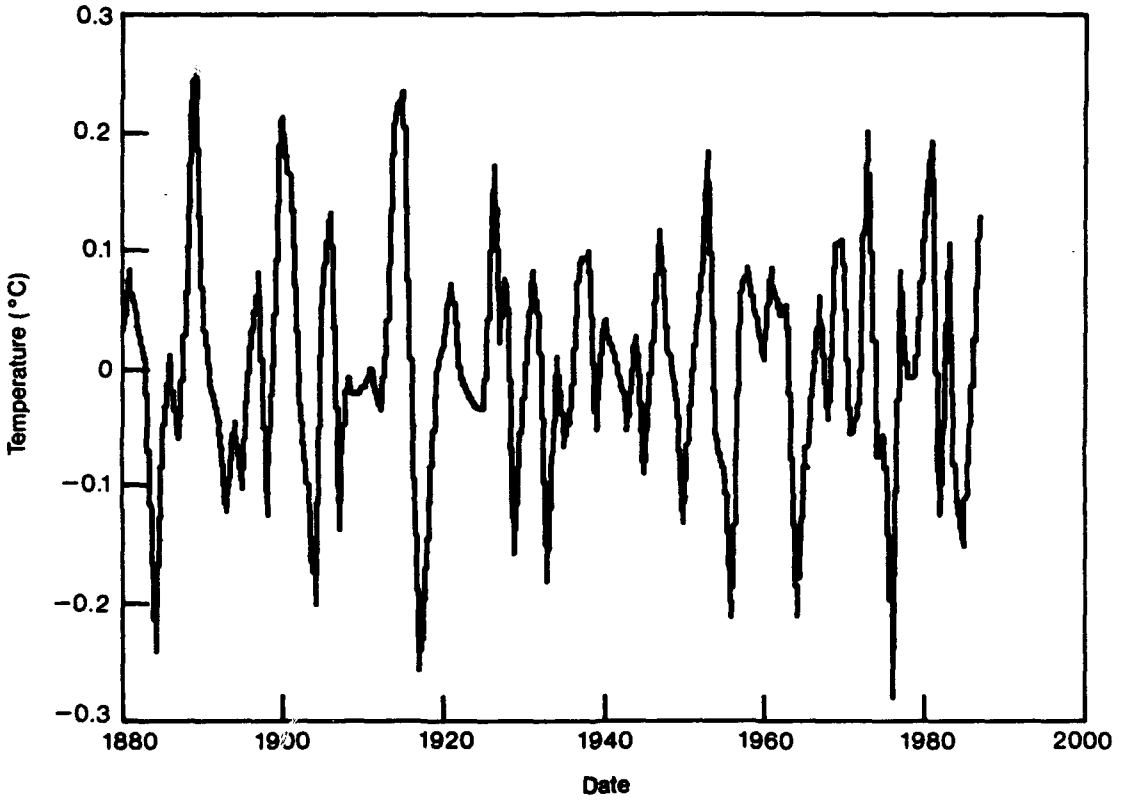

Figure 9. The residual variations in global annual average surface temperature after removing the low-frequency variations (Figure 8) and a linear trend from the record shown in Figure 1.

An important issue is whether the low frequency components represent chaotic "noise" or whether they represent low frequency processess with well defined time scales, possibly of oceanic origin. The data available are insufficient to provide an answer though the arguments summarized above on the statistical distribution of the data favor the chaotic noise hypothesis.

Similar presentations of the data for the Jones global, annual average surface air temperature sets (see Figure 3) are shown in Figures 10 and 11. The low frequency variations show great similarity to those observed in the Hansen-Lebedeff series (see Figure 8). Figure 12 shows the high degree of correlation between the low frequency components of the Hansen-Lebedeff series and the Jones series over the peirod of overlap of the records, 1880-1987. The high correlation is perhaps surprising in that there is only a partial overlap in the data sets. Only the data derived from land-based meterological stations are present in both data sets; the Jones data set relies heavily on ocean observations.

Given the large amplitude of the low frequency variation, at least a partial prediction of future global surface air temperature is possible. The low frequency components can be extrapolated, for example, using the Fourier expansion of the observed data and adding the linear trend of 0.55°C/century. This procedure provide the basis for forecasting the future low frequency variability to which must be added the high frequency "noise" which must be dealt with statistically. The observed data suggest that in the next few years, the low frequency variation will act, in part, to reduce the linear increasing trend though the actual temperatures reached in any individual year will be dependent on the high frequency noise.

As our final data set we use the longest surface air temperature record

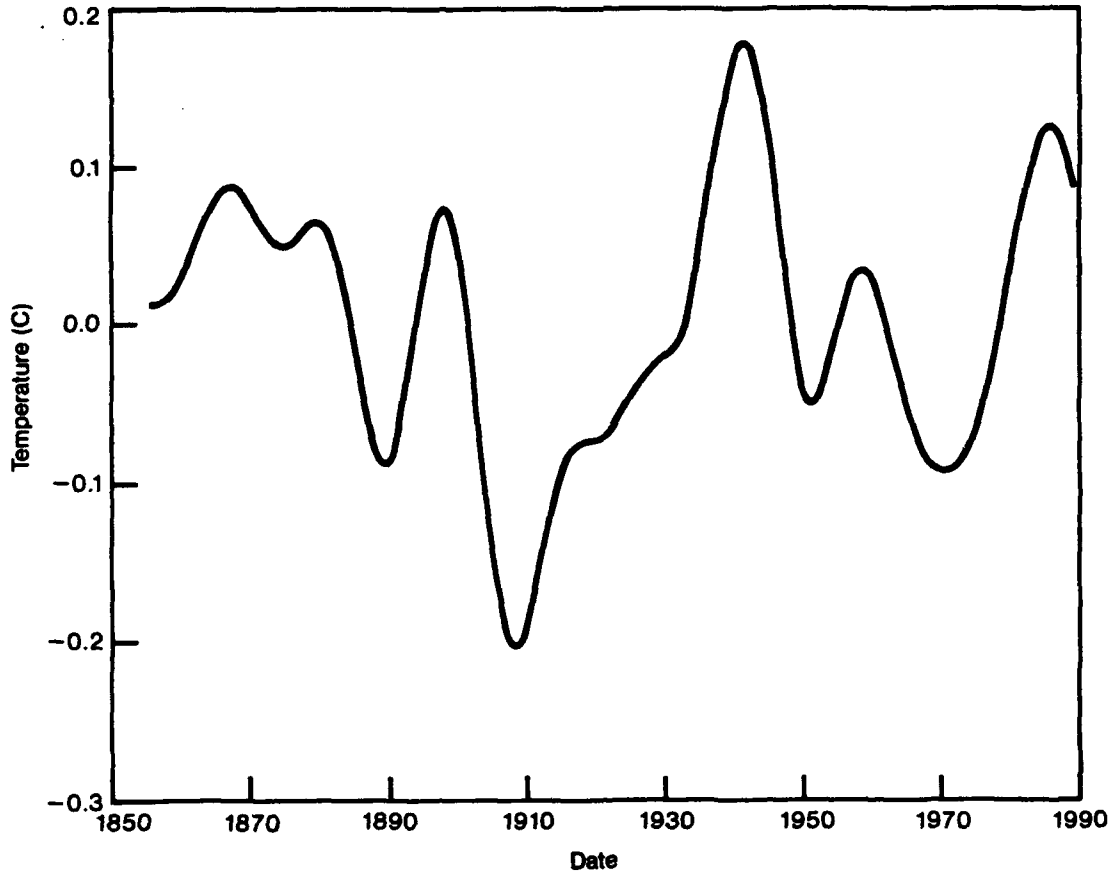

Figure 10. The low-frequency (< 0.04 cpyr) components of the global annual average surface air temperature prepared by Jones (1988, and personal communication, 1990). (See Figure 3.)

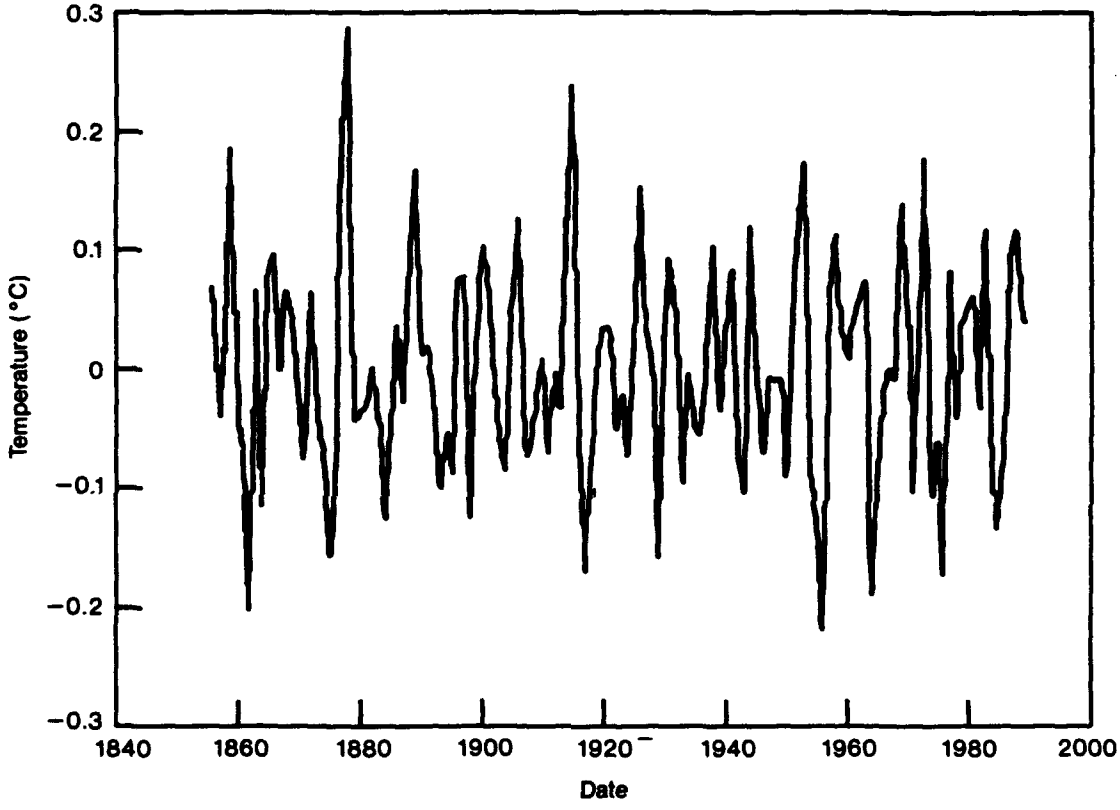

Figure 11. The residual temperature variations obtained after removing the low-frequency components (Figure 10) and a linear trend from the global annual average surface air temperature record given in Figure 3.

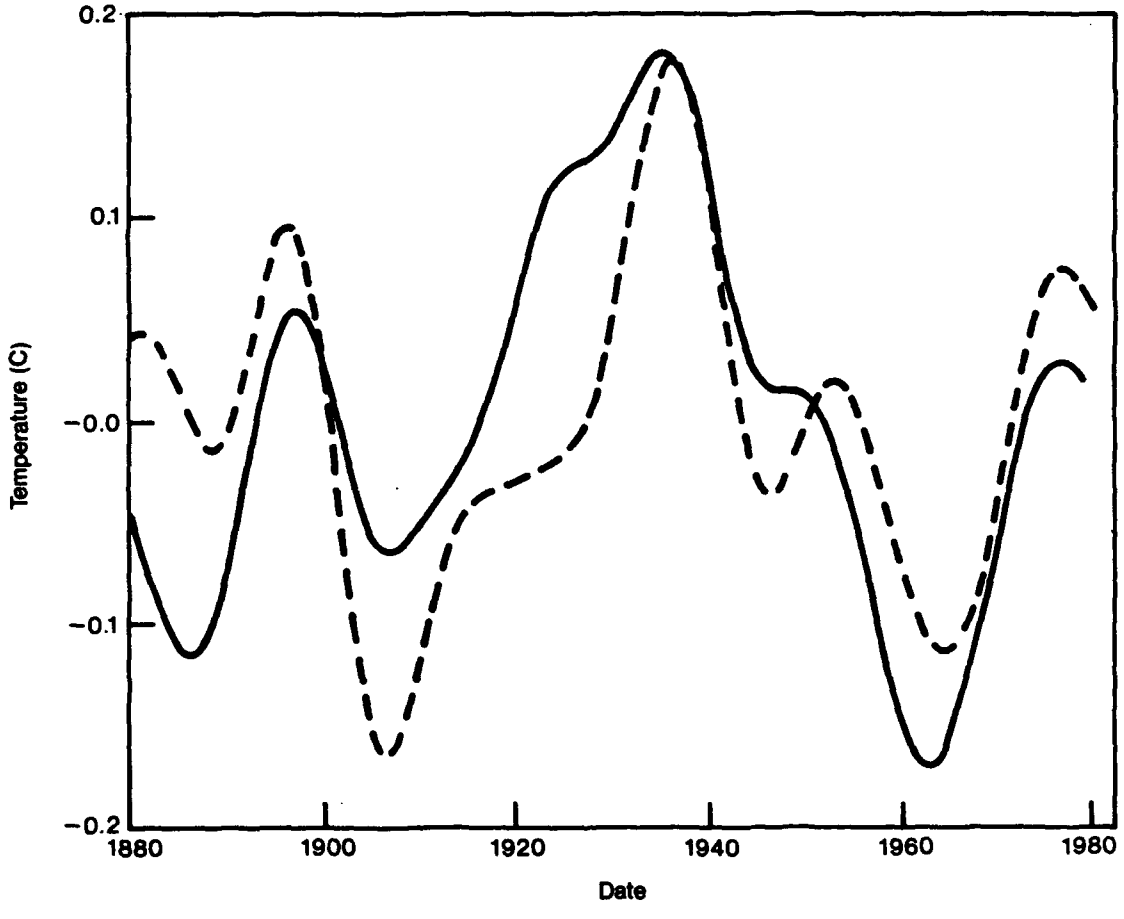

Figure 12. Comparison of the low-frequency (< 0.04 cpyr) components of the Hansen-Lebedeff (Figure 1) and the Jones (Figure 3) records. The solid line corresponds to the Hansen-Lebedeff record.

available to us; the temperature record compiled by Manley (1974) for Central England. This record differs from the Jones and Hansen-Lebedeff records in that it is in effect a single station. Manley (1974) pieced together the early part of the series from notebooks kept by amateur observers in various parts of England and Scotland. Making different corrections for station location, Manley constructed a single record that represents of Central England over three centuries. Figure 13 shows the Manley record with its high level of noise. The power spectrum for the Manly record is shown in Figure 14, and clearly, there is less energy in the low-frequency components than in the global average temperature records (see Figure 2 and 4). The spatial averaging used in obtaining global averages reduces the high-frequency content of the resulting records and raises the low frequency components. The low-frequency part of the Manley record is displayed in Figure 15 and the residuals obtained after the removal of the low-frequencies and a linear trend is shown in Figure 16. Again the issue is whether this long term variability is due to chaotic motion or to predictable long-term changes in ocean circulation. Of particular interest in Figure 15 is the strong minimum in the temperature curve between 1690 and 1700. This period was the minimum in temperatures during the Little Ice Age. A long-term swing downward carried the high frequency variations into an extended period of cold weather, leading to the disastrous climate conditions that devastated all of Northern Europe in the late 1600s. The peak to peak variations in the low-frequency variations are somewhat greater than 2°C, while the high-frequency noise terms have peak to peak amplitude greater than 3°C. These are a factor of 6 to 7 greater than the global average records.

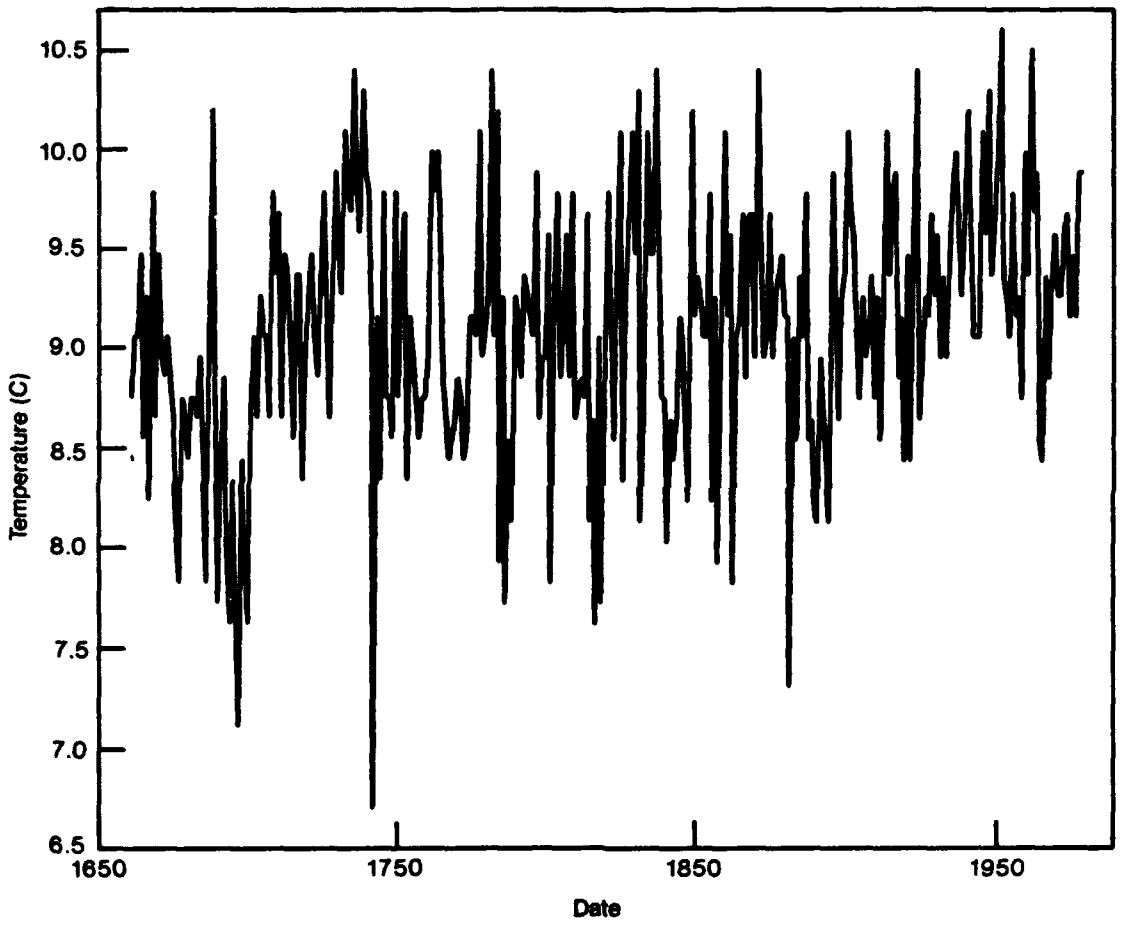

Figure 13. Variations in yearly average temperature in Central England, after Manley (1974).

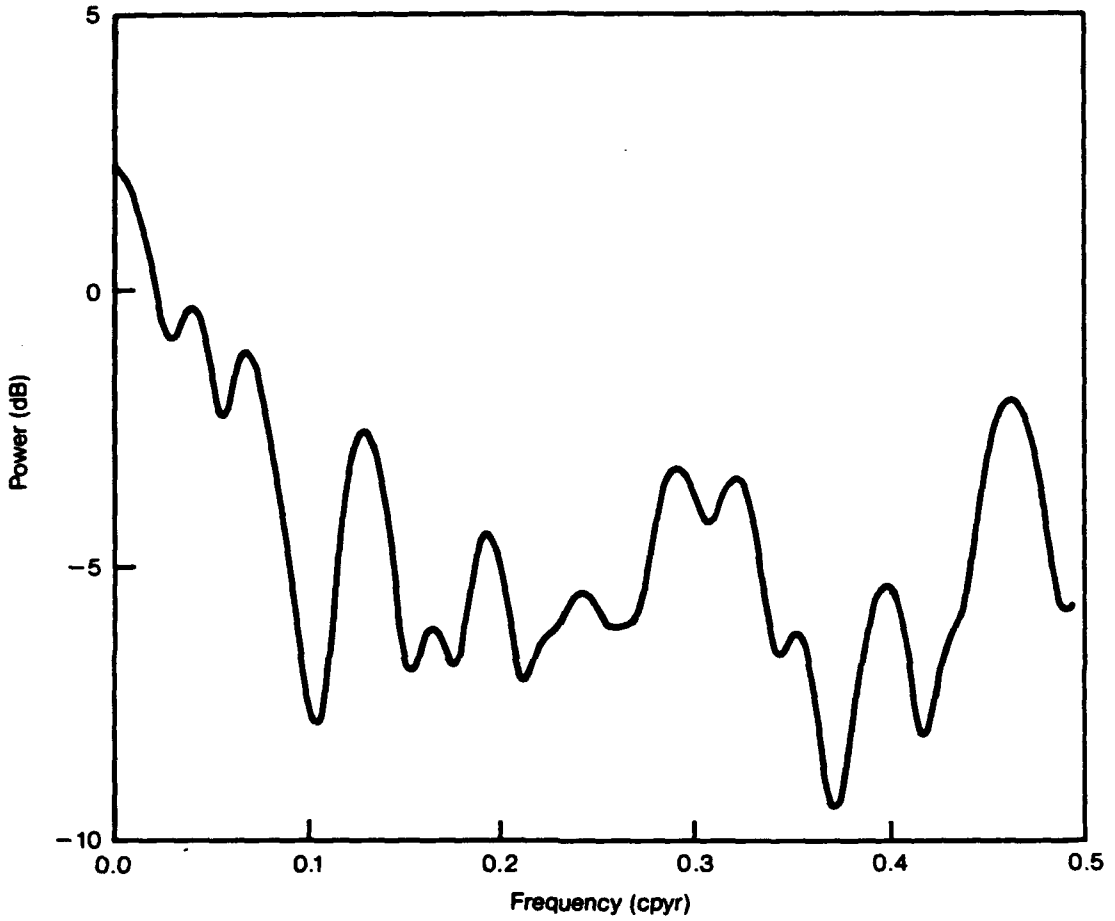

Figure 14. Power spectrum of the Manley temperature record for Central England shown in Figure 13. The data have been normalized to zero mean and unit variance for ease of comparison with Figures 2 and 4.

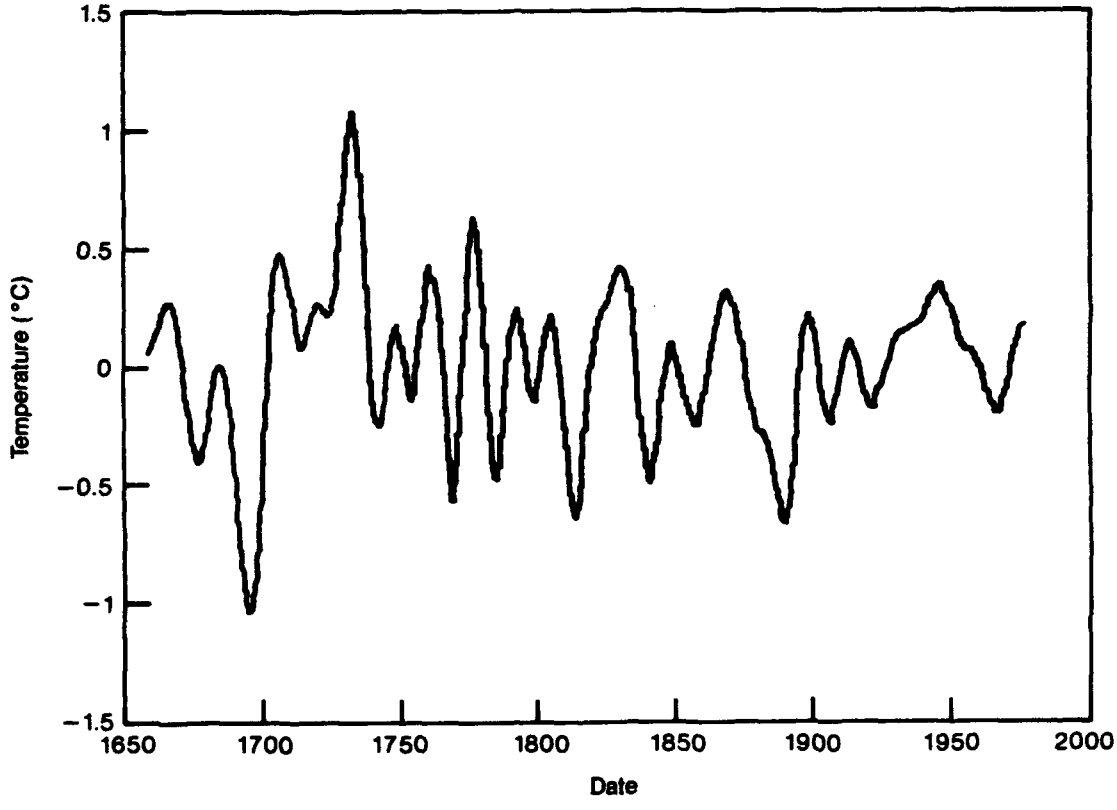

Figure 15. The low-frequency (< 0.04 cpyr) components of the Manley temperature curve for Central England (see Figure 13).

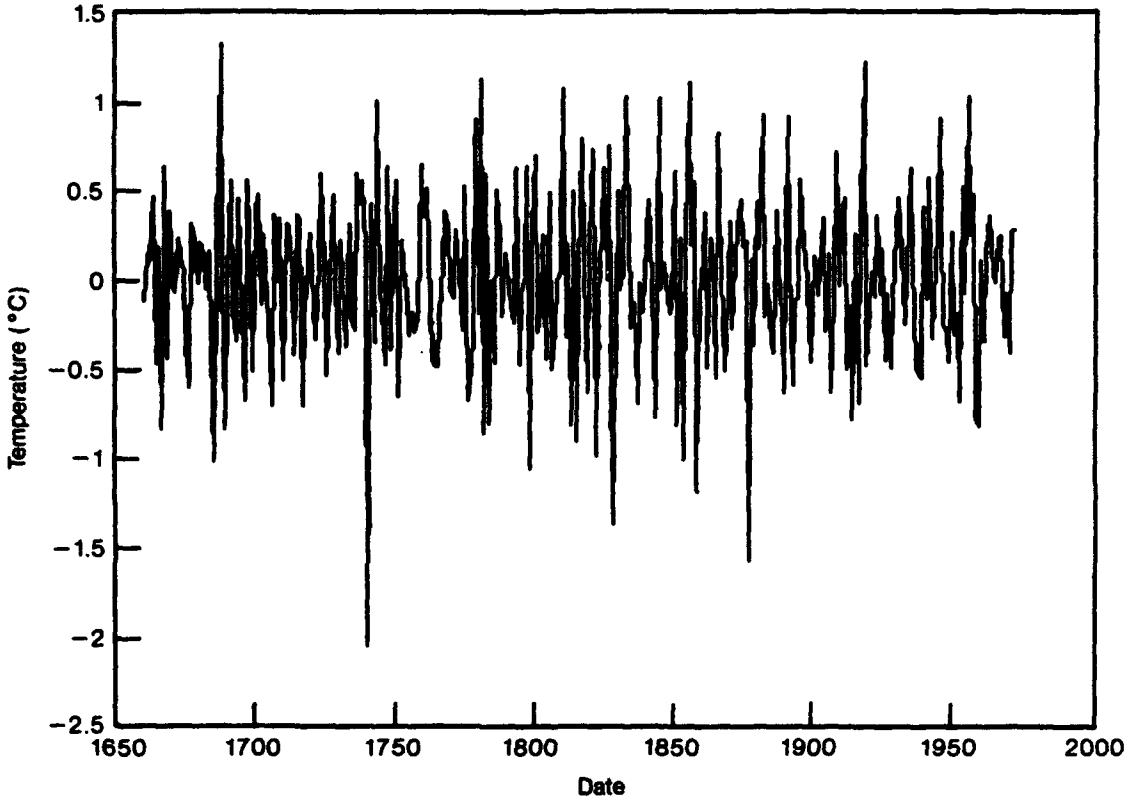

Figure 16. The residuals in the temperature curve after removal of the low-frequency terms (see Figure 15) and a linear trend from the Manley temperature record shown in Figure 13.

6.3 Model Results

The low-frequency variations of the Lorenz 27-variable model (see Figures 5 and 6) are shown in Figure 17. In this case there can be no question that the long-term fluctuations illustrated by Figure 17 are of chaotic origin. The model contains a "swamp" representation of the ocean. The ocean responds to temperature changes by varying rates of evaporation and liquid water returns to the ocean through precipitation. There is no circulation within the ocean; therefore, "predictable" long-term ocean-driven changes are ruled out. If any 100-year section of Figure 17 is compared with the low frequency variations shown by global average surface temperature (Figures 10 and 12), there is a close resemblance except that the peak to peak amplitude in the model is significantly greater than in the global average data record. This differences arises, in part, from the fact that the Lorenz model temperatures correspond to a station value (see Figure 15) rather than to spatially averaged values. In that way they are more like the Manley records.

The residual variations in temperature after removing the low-frequency components (Figure 17) from the Lorenz 27-variable model (see Figure 5) are displayed in Figure 18. The high-frequency chaotic noise resembles white motion and shows a peak to peak amplitude of 1.3°C, less than the peak to peak amplitude of the low-frequency components.

6.4 Summary of Data Record and Model Runs

Both the data sets and the model runs show high-amplitude low-frequency variations. Among the data sets, the globally averaged records show a higher fraction of the variance in the low-frequencies than in a record from a single

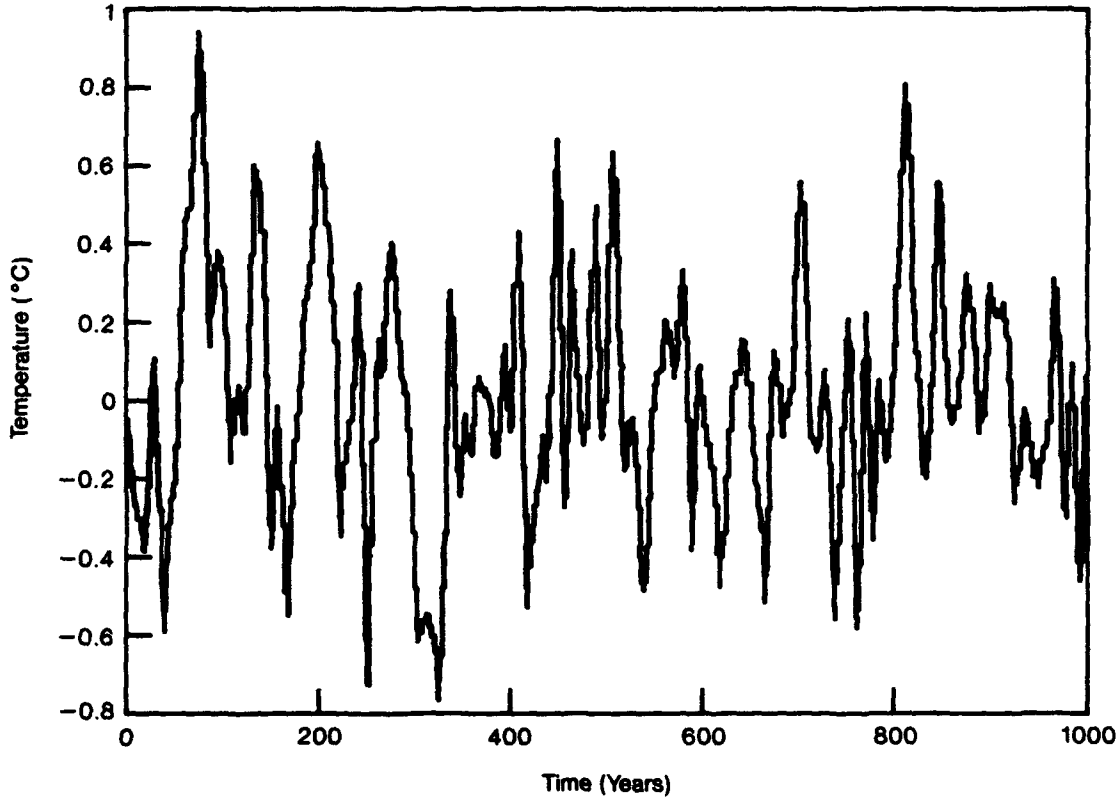

Figure 17. The low-frequency components (< 0.04 cpyr) of the Lorenz 27-variable model run (see Figure 5).

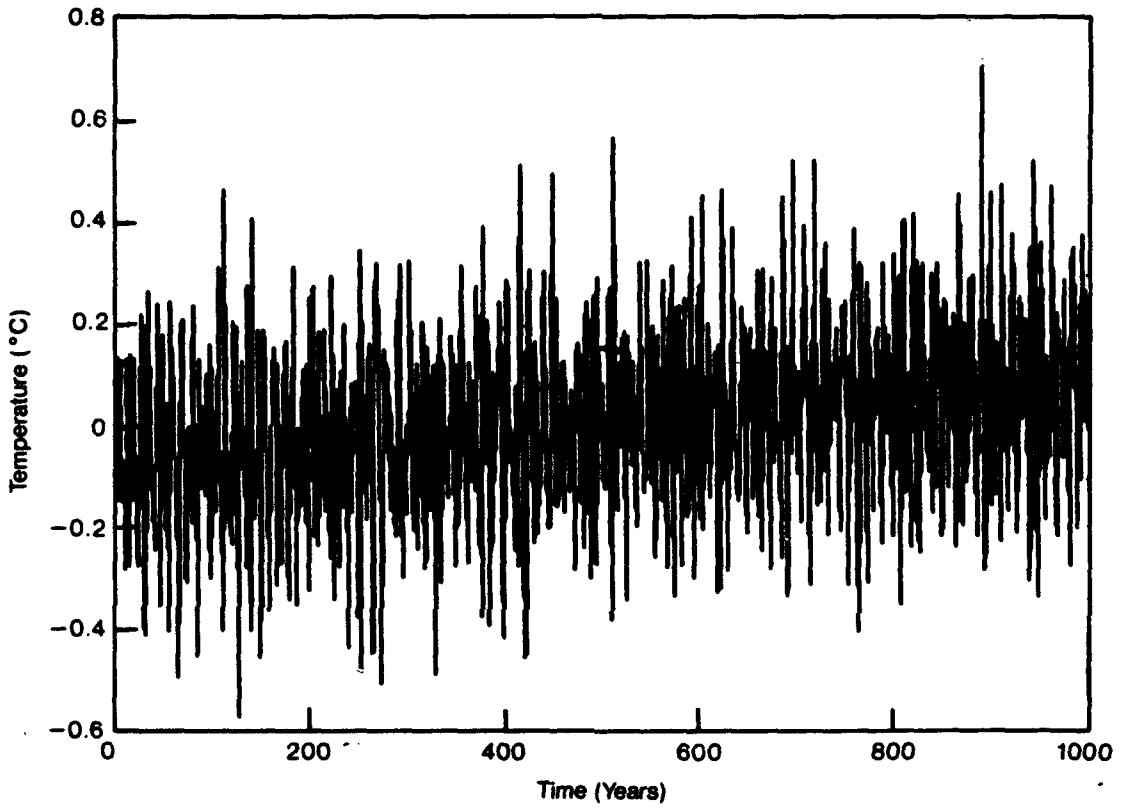

Figure 18. Residual variations in temperature for the Lorenz 27-variable model (see Figure 5) after removal of the low-frequency components (see Figure 17).

location (Manley temperature record). The Lorenz 27-variable model contains a larger fraction of the total variance in the low frequency components. In the Lorenz case, all the variance is due to chaotic noise. The observational data sets are, of course, contaminated by observational evolution. This contaminating noise in the observational data may have the effect of raising the high-frequency part of the spectrum. This kind of contamination has certainly affected the Manley record (see Figure 13).

A summary of the distribution of variance among the various components is shown in Table 1. For the global average surface air temperature the low-frequency components (linear trend and variations below 0.04 cpyr) contain about 50% of the variance. In the model results, 72% of the variance is in the low-frequency fluctuations, and these fluctuations are of chaotic origin.

6.5 Phase Plot Representation of Low-Frequency Components in Data Sets and Model Runs

The number of values in the observed data sets discussed above is much too small to obtain a reliable estimate of the fractal or of the correlation dimension of the attractor, if one exists. An alternative scheme is to examine the eigenvalue structure of the correlation matrix under various assumptions as to the embedding dimension and in this way obtain an estimate of the attractor dimension. The procedure is illustrated in Figure 19, where the magnitudes of the eigenvalues for the Hansen-Lebedeff temperature curve filtered at 0.04 cpyr (see Figure 8) are shown for embedding dimension 5, 10 and 20. For embedding dimensions 5, one or possibly two eigenvalues dominate, while for embedding dimension 20, the first three eigenvalues appear dominant, suggesting an attractor with dimension of about three.

Table 1
Distribution of Variance in Temperature Records

Record	Length (Years)	Slopes of Trend (°C/Century)	Percentage of Variance in Various Components		
			Linear Trend	Low Frequency (<0.04 cpyr)	High Frequency (>0.04 cpyr)
Hansen-Lebedeff (see Figure 1)	108	0.55	37.3	10.7	52.0
Jones (see Figure 3)	134	0.28	30.3	17.6	52.1
Manley (see Figure 13)	318	0.19	7.1	28.2	64.7
Lorenz Model (see Figure 5)	1000	—	—	72.2	27.8

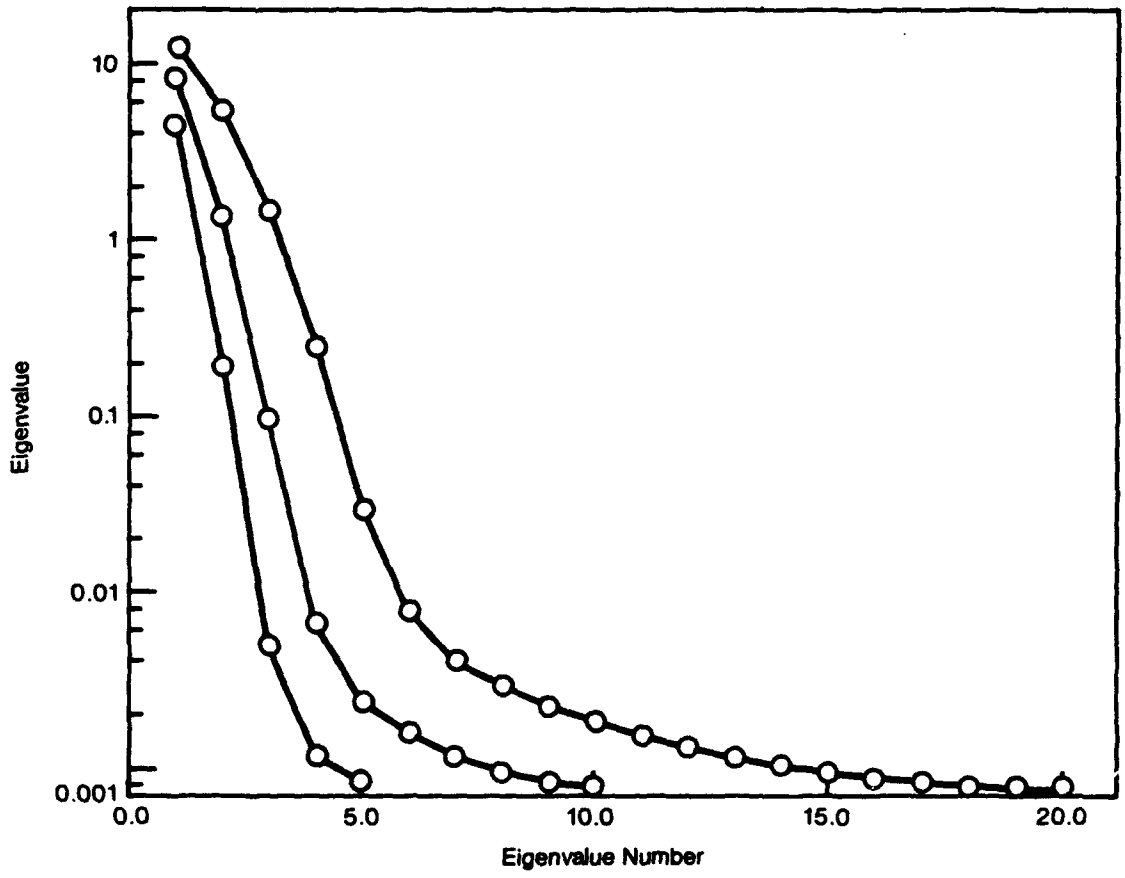

Figure 19. Eigenvalues for the correlation matrix of the Hansen-Lebedeff temperature curve (Figure 1) filtered at 0.04 cpyr (see Figure 8) at embedding dimensions 5, 10 and 20.

The structure of the eigenvectors of the correlation matrix shows that the first principal component for embedding dimension 5 corresponds to a running average of five values, while the second principal component corresponds to the running difference across the five values. A plot of the filtered temperature curve in the plane defined by the first two principal component axes is then basically a phase plot of the change in temperature graphed against the temperature. Figure 20 shows the phase plot for the 108 year long Hansen-Lebedeff temperature curve. The cusps in the curve undoubtedly represent the fact that two dimensions are insufficient to capture the full structure of the three- dimensional motion.

The above procedure can be tested by examining the Lorenz 27-variable surface air temperature model. The correlation dimension for the model run filtered at 0.04 cpyr is about 4 (see Figure 7). The eigenvalue structure for the correlation matrix of the Lorenz 27-variable model is given in Figure 21. The first four eigenvalues dominate for embedding dimension 20, leading to an estimated attractor dimension of 4 in agreement with the estimated correlation dimension. The phase plot for the filtered (at 0.04 cpyr) Lorenz 27-variable surface air temperature record is given in Figure 22. The phase plot (for 300 years) shows considerably more structure than the Hansen-Lebedeff curve, which is not unexpected given the higher fraction of the total variance in the low-frequency region of the model as contrasted to the data (see Table 1). Further filtering of the data to 0.02 cpyr simplifies the phase plot considerably (see Figure 23). Whether conventional or newer nonlinear dynamics methods of prediction could be applied to these representations remain to be tested.

Figure 24 shows a phase plot of normally distributed random noise filtered at 0.04 cpyr. The similarity between the phase plot for low-frequency noise

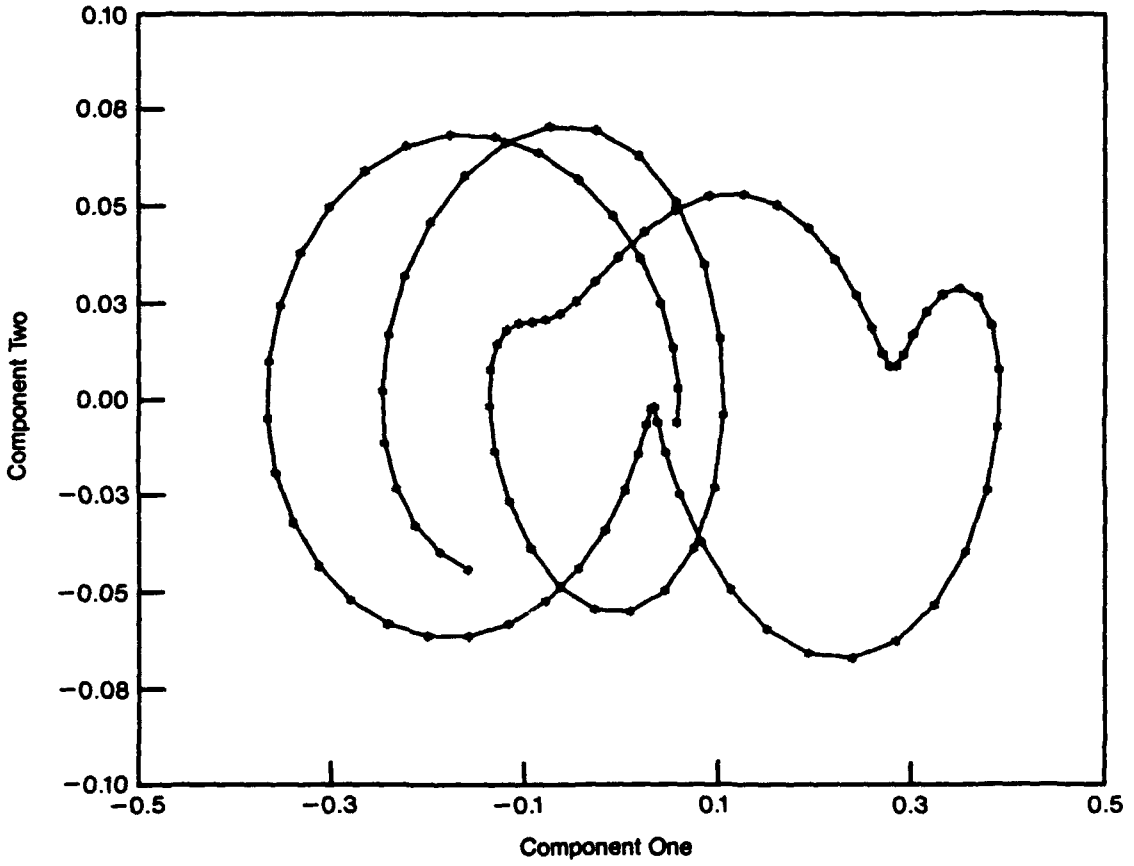

Figure 20. Filtered (at 0.04 cpyr) Hansen-Lebedeff temperature curve (see Figure 8) plotted against the first two principal components. As discussed in the text, the graph is a phase plot of the average change in temperature (component 2) graphed against average temperature (component 1).

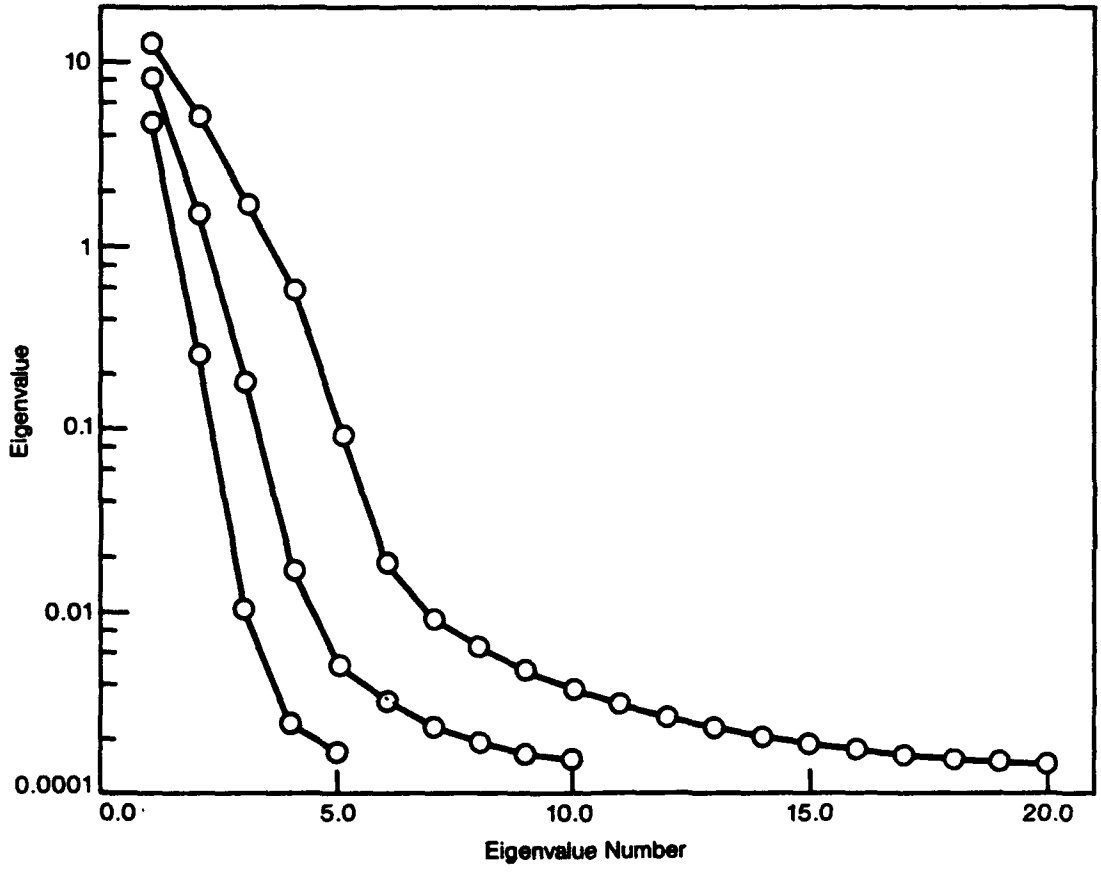

Figure 21. Eigenvalue for the correlation matrix at various embedding dimensions for the Lorenz 27-variable model of surface air temperature filtered at 0.04 cpyr. The correlation dimension for such a record is 4 (see Figure 7).

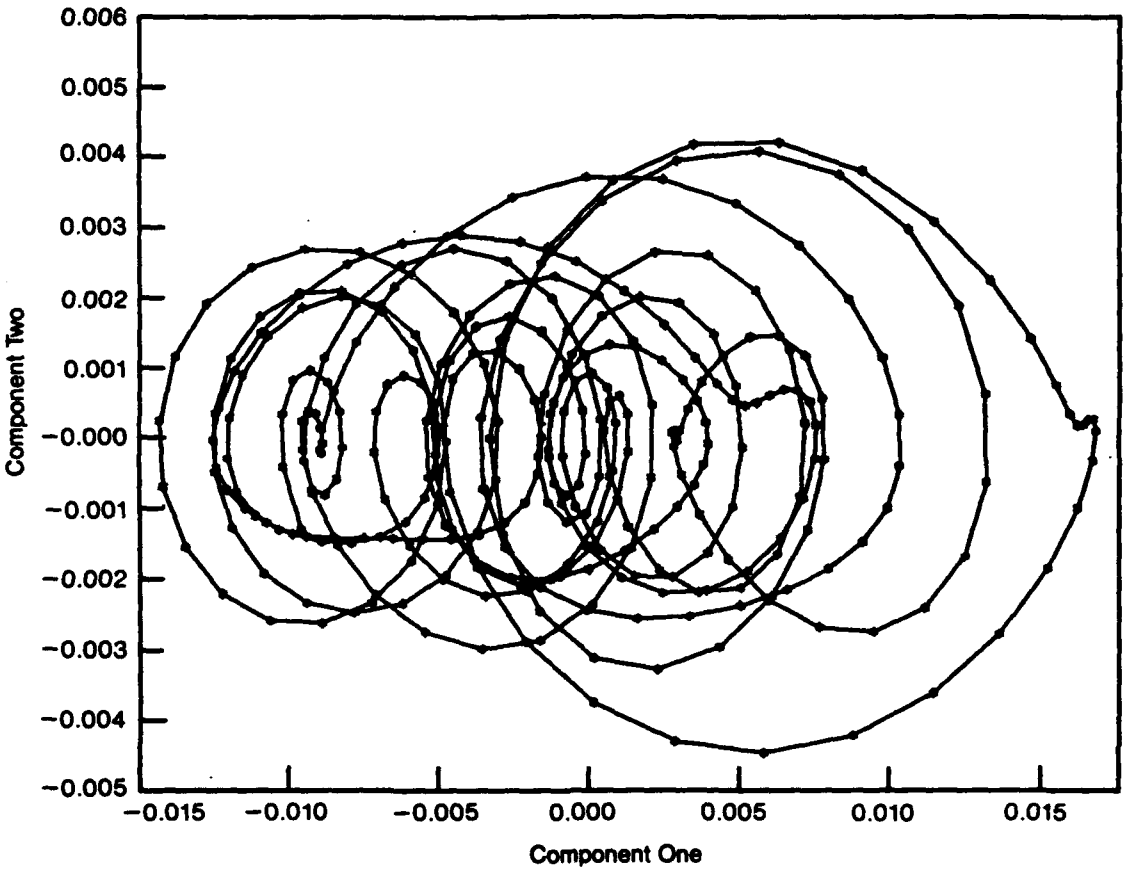

Figure 22. Phase plot for the Lorenz 27-variable model for surface air temperature filtered at 0.04 cpyr. Component one corresponds to the five-year running average temperature and component two is the five-year average derivative of temperature. This plot combines 350 years of the record.

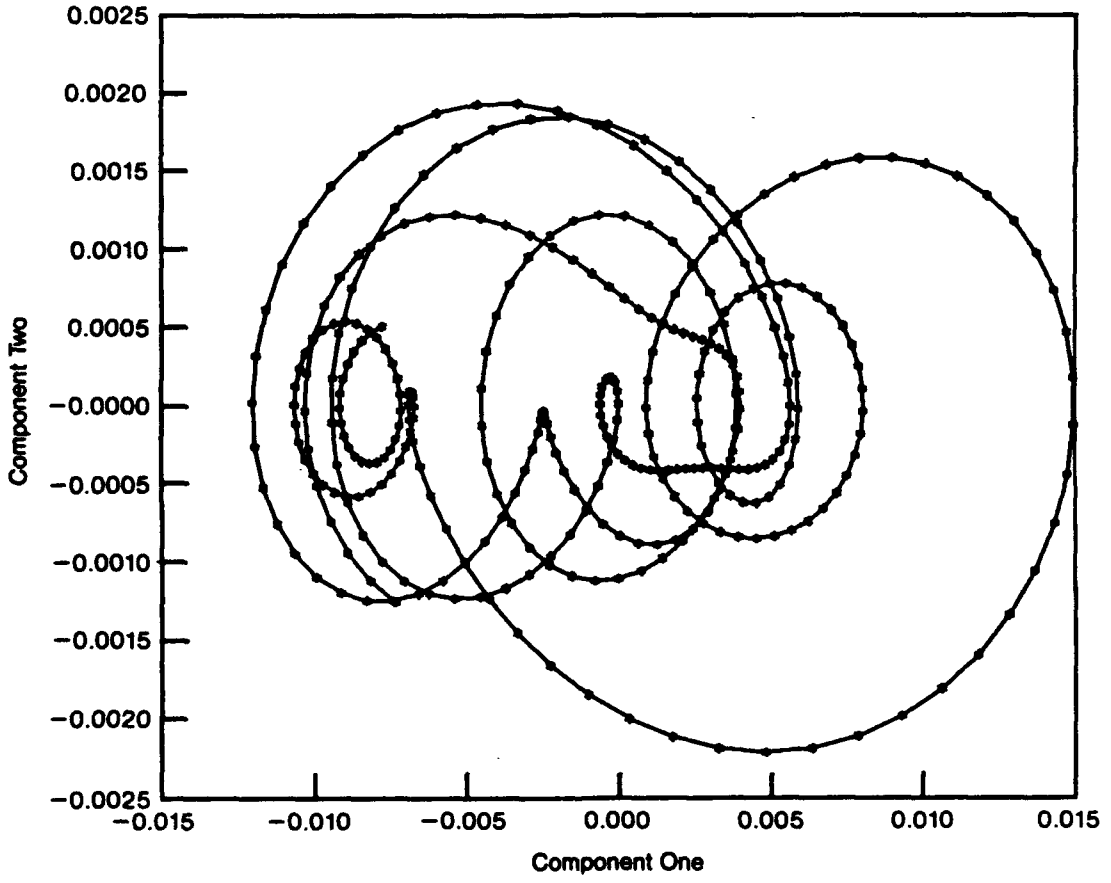

Figure 23. Phase plot for the Lorenz 27-variable model surface air temperature filtered at 0.02 cpyr (see Figure 20).

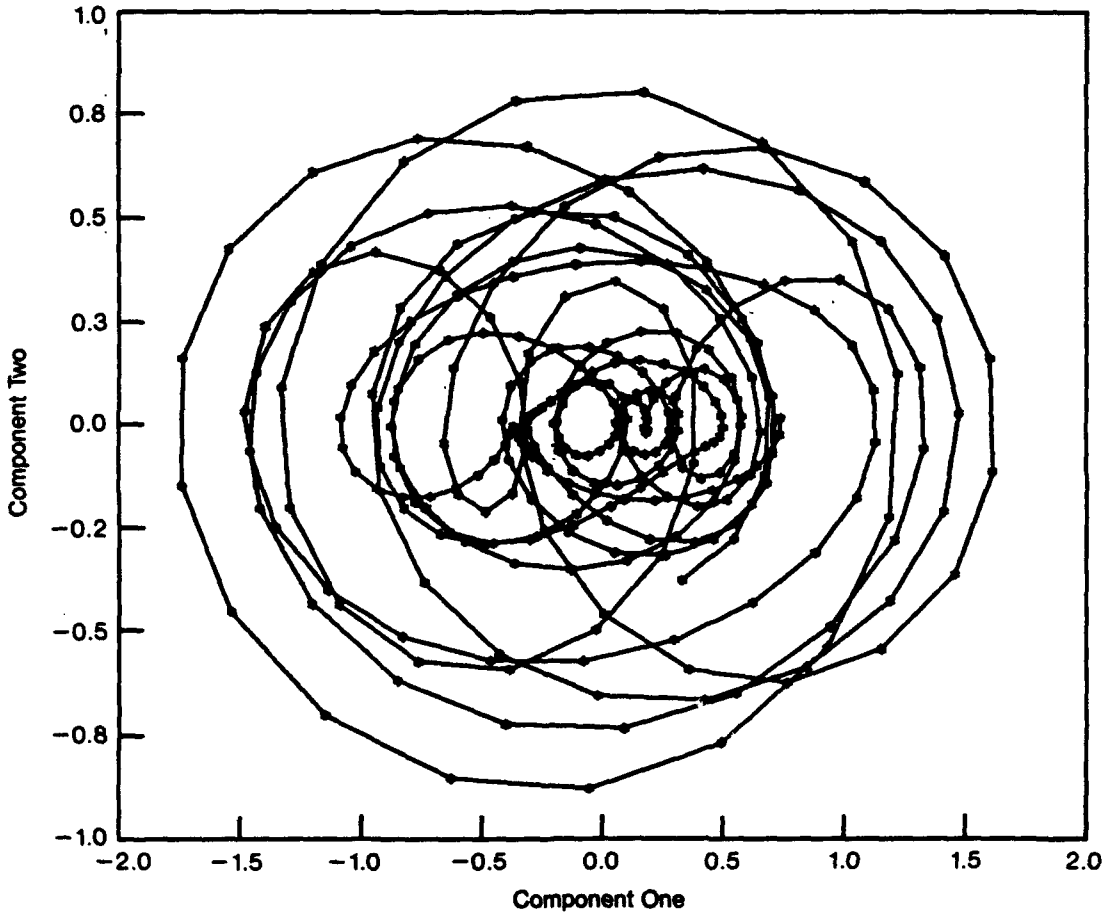

Figure 24. Phase plot for normally distributed noise, as a model of climate, filtered at 0.04 cpyr.

and that for the Lorenz 27-variable attractor is not surprising, since the values generated by the Lorenz 27-variable model for surface air temperature closely approximate those of a normally distributed random variable (see Sections 2 and 4).

The eigenvalue structure for the Manley temperature record (318 years) filtered at 0.04 cpyr is displayed in Figure 25. It would appear that four and possibly five eigenvalues are significant so that four-five dimensions are required to depict the attractor. The phase plot for the Manley record (see Figure 24) show a complex structure similar to that of the Lorenz 27-variable model (see Figure 21). Whether the Manley record at low frequency represents chaotic motion or an underlying predictable signal remains an unanswered question.

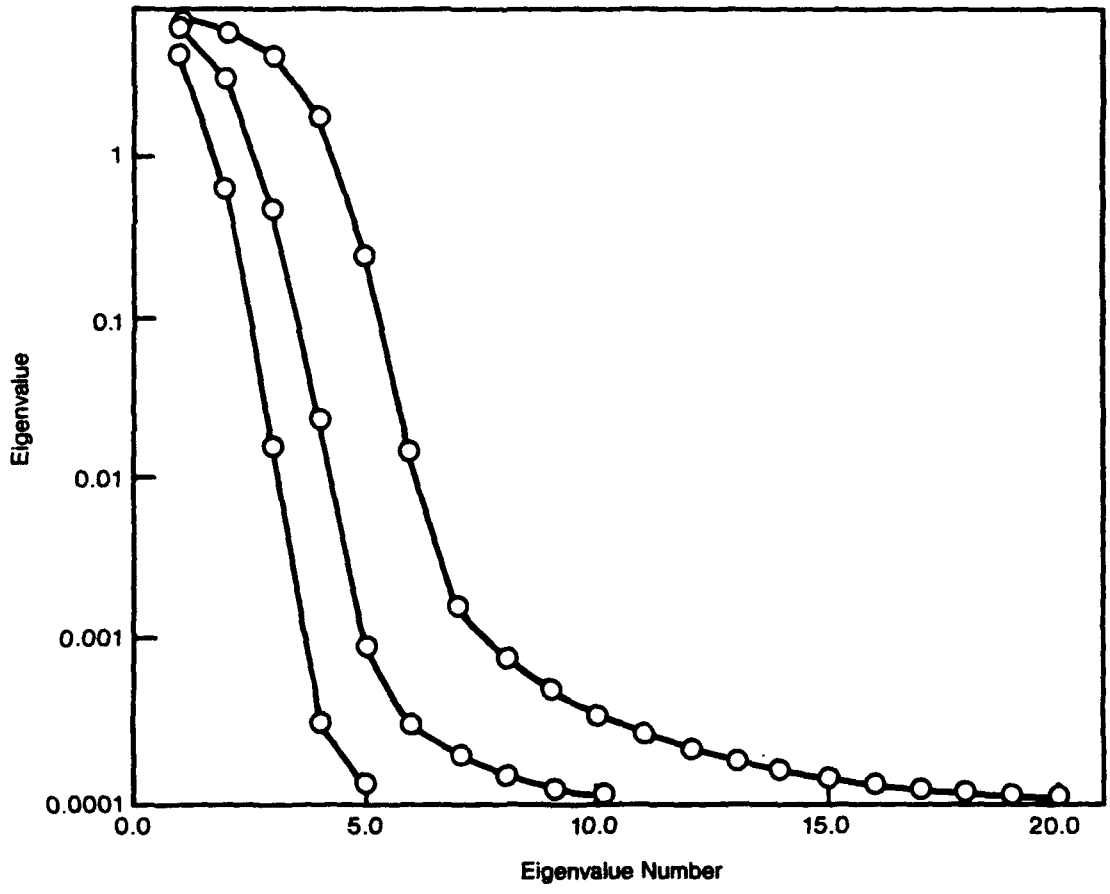

Figure 25. The eigenvalue structure for the correlation matrix at various embedding dimensions for the filtered (at 0.04 cpyr) Manley temperature record for Central England (see Figure 15).

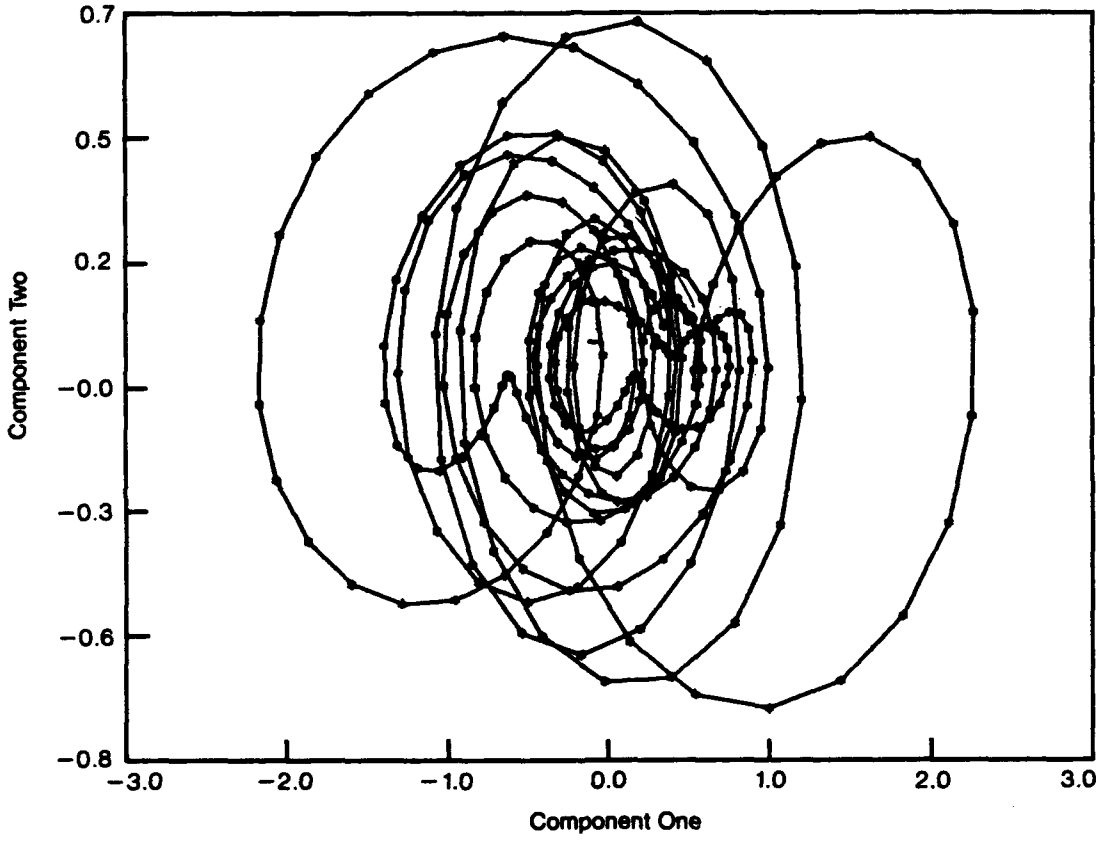

Figure 26. Phase plot for the Manley temperature record for Central England filtered at 0.04 cpyr.

7 SUMMARY COMMENTS

The question as to the origin of the low-frequency components in climate records – chaotic motion or predictable fluctuations – remains open. Statistical analyses of data sets and of low-order climate models strongly suggest that the low-frequency components are chaotic, but this hypothesis has not been tested on Global Circulation Models. Such tests are essential if progress is to be made with respect to the question: Is climate predictable?

The theory of prediction for low-order dynamical systems is still in its infancy, but may have important applicability to the problems of short-term climate prediction. Developments in the field of nonlinear predictability should be closely watched since this is a rapidly growing area of nonlinear dynamics.

We have emphasized the reduction of the attractor dimension by averaging in order to increase the prospects for prediction. The results obtained from long runs of GCMs should be tested along the lines described in this report in order to investigate the extent to which climate is predictable.

Our report deals only with temporal averaging. Many of the questions raised by examining temporal averaging are relevant to the question of spatial averaging. The issues need to be investigated in three-dimensional models to better define the length scales over which prediction is possible.

REFERENCE

1. Abarbanel, H., H. Levine, G. MacDonald and O. Rothaus (1990) Statistics of Extreme Events with Application to Climate, JASON (JSR-90-305), MITRE, McLean, VA.

2. Abarbanel, H. (1990) Prediction in chaotic nonlinear systems: Time series analysis for aperiodic evolution, in *Global Climate and Ecosystem Change*, ed. by G. MacDonald and L. Sertorio, Plenum Press, New York

3. Hansen, J. and S. Lebedeff (1987) Global trends of measured surface air temperature, *J. Geophys. Res.*, **92**, 13345-13372

4. Hansen, J. and S. Lebedeff (1988) Global surface temperature; Update through 1987, *Geophys. Res. Letters*, **15**, 323-326

5. Hasselmann, K. (1976) Stochastic climate models, Part 1: Theory, *Tellus*, **28**, 473-485

6. Jones, P. (1988) Hemispheric surface air temperature variation recent trends and an update, *J. Clim*, **1**, 654-660

7. Lorenz, E. (1963) The predictability of hydrodynamic flow, *Trans. N. Y. Acad. Sci, Ser 2*, **25**, 409-432

8. Lorenz, E. (1969) Atmospheric predictability as revealed by naturally occurring analogues, *J. Atmos. Sci*, **26**, 636-646

9. Lorenz, E. (1976) Nondeterministic theories of climate change, *Quart. Res*, **6**, 495-506

10. Lorenz, E. (1984a) Irregularity: a fundamental property of the atmosphere, *Tellus*, **36A**, 98-110

11. Lorenz, E. (1984b) Formulation of a low-order model of a moist general circulation model, *J. Atmos. Sci*, **41**, 1933-1945

12. Manley, G. (1974) Central England temperatures: Monthly means 1659-1973, *Quart. J. Roy. Meteor. Soc*, **100**, 389-405

DISTRIBUTION LIST

Dr Henry D I Abarbanel
Institute for Nonlinear Science
Mail Code R002/Building CMRR/Room 115
University of California/San Diego
La Jolla, CA 92093-0402

Director Ames Laboratory [2]
Iowa State University
Ames, IA 50011

Mr John M Bachkosky
Deputy DDR&E
The Pentagon
Room 3E114
Washington, DC 20301

Dr Joseph Ball
Central Intelligence Agency
Washington, DC 20505

Dr Arthur E Bisson
DASWD (OASN/RD&A)
The Pentagon
Room 5C675
Washington, DC 20350-1000

Dr Albert Brandenstein
Chief Scientist
Office of Natl Drug Control Policy
Executive Office of the President
Washington, DC 20500

Mr Edward Brown
Assistant Director
Nuclear Monitoring Research Office
DARPA
3701 North Fairfax Drive
Arlington, VA 22203

Dr Herbert L Buchanan III
Director
DARPA/DSO
3701 North Fairfax Drive
Arlington, VA 22203

Dr Curtis G Callan Jr
Physics Department
PO Box 708
Princeton University
Princeton, NJ 08544

Dr Ferdinand N Cirillo Jr
Central Intelligence Agency
Washington, DC 20505

Brig Gen Stephen P Condon
Deputy Assistant Secretary
Management Policy &
Program Integration
The Pentagon Room 4E969
Washington, DC 20330-1000

Ambassador Henry F Cooper
Director/SDIO-D
Room 1E1081
The Pentagon
Washington, DC 20301-7100

DISTRIBUTION LIST

DARPA
RMO/Library
3701 North Fairfax Drive
Arlington, VA 22209-2308

Mr John Darrah
Senior Scientist and Technical Advisor
HQAF SPACOM/CN
Peterson AFB, CO 80914-5001

Col Doc Dougherty
DARPA/DIRO
3701 North Fairfax Drive
Arlington, VA 22203

DTIC [2]
Defense Technical Information Center
Cameron Station
Alexandria, VA 22314

Mr John N Entzminger
Director
DARPA/TTO
3701 North Fairfax Drive
Arlington, VA 22203

CAPT Kirk Evans
Director Undersea Warfare
Space & Naval Warfare Sys Cmd
Code PD-80
Department of the Navy
Washington, DC 20363-5100

Dr Dave Galas
Associate Director for
Health & Environmental Research
ER-70/GTN
US Department of Energy
Washington, DC 20585

Dr S William Gouse
Sr Vice President and General Manager
The MITRE Corporation
Mail Stop Z605
7525 Colshire Drive
McLean, VA 22102

LTGEN Robert D Hammond
CMDR & Program Executive Officer
US Army/CSSD-ZA
Strategic Defense Command
PO Box 15280
Arlington, VA 22215-0150

Mr Thomas H Handel
Office of Naval Intelligence
The Pentagon
Room 5D660
Washington, DC 20350-2000

Maj Gen Donald G Hard
Director of Space and SDI Programs
Code SAF/AQS
The Pentagon
Washington, DC 20330-1000

Dr Robert G Henderson
Director
JASON Program Office
The MITRE Corporation
7525 Colshire Drive Z561
McLean, VA 22102

DISTRIBUTION LIST

Dr Barry Horowitz
President and Chief Executive Officer
The MITRE Corporation
Burlington Road
Bedford, MA 01730

Dr William E Howard III [2]
Director For Space
and Strategic Technology
Office/Assistant Secretary of the Army
The Pentagon Room 3E474
Washington, DC 20310-0103

Dr Gerald J Iafrate
US Army Research Office
PO Box 12211
4300 South Miami Boulevard
Research Triangle Park, NC 27709-2211

Technical Information Center [2]
US Department of Energy
PO Box 62
Oak Ridge, TN 37830

JASON Library [5]
The MITRE Corporation
Mail Stop W002
7525 Colshire Drive
McLean, VA 22102

Dr George Jordy [25]
Director for Program Analysis
US Department of Energy
MS ER30 Germantown
OER
Washington, DC 20585

Dr O'Dean P Judd
Los Alamos National Lab
Mail Stop A-110
Los Alamos, NM 87545

Dr Steven E Koonin
Kellogg Radiation Laboratory
106-38
California Institute of Technology
Pasadena, CA 91125

Dr Herbert Levine
Department of Physics
Mayer Hall/B019
University of California/San Diego
La Jolla, CA 92093

Technical Librarian [2]
Argonne National Laboratory
9700 South Cass Avenue
Chicago, IL 60439

Research Librarian [2]
Brookhaven National Laboratory
Upton, NY 11973

Technical Librarian [2]
Los Alamos National Laboratory
PO Box 1663
Los Alamos, NM 87545

DISTRIBUTION LIST

Technical Librarian [2]
Pacific Northwest Laboratory
PO Box 999
Battelle Boulevard
Richland, WA 99352

Technical Librarian [2]
Sandia National Laboratories
PO Box 5800
Albuquerque, NM 87185

Technical Librarian [2]
Sandia National Laboratories
PO Box 969
Livermore, CA 94550

Technical Librarian [2]
Lawrence Berkeley Laboratory
One Cyclotron Road
Berkeley, CA 94720

Technical Librarian [2]
Lawrence Livermore Nat'l Lab
PO Box 808
Livermore, CA 94550

Technical Librarian [2]
Oak Ridge National Laboratory
Box X
Oak Ridge, TN 37831

Chief Library Branch [2]
AD-234.2 FORS
US Department of Energy
Washington, DC 20585

Dr Gordon J MacDonald
Institute on Global Conflict
& Cooperation
UCSD/0518
9500 Gilman Drive
La Jolla, CA 92093-0518

Mr Robert Madden [2]
Department of Defense
National Security Agency
Attn R-9 (Mr Madden)
Ft George G Meade, MD 20755-6000

Dr Arthur F Manfredi Jr [10]
OSWR
Central Intelligence Agency
Washington, DC 20505

Mr Joe Martin
Director
OUSD(A)/TWP/NW&M
Room 3D1048
The Pentagon
Washington, DC 20301

Dr Julian C Nall
Institute for Defense Analyses
1801 North Beauregard Street
Alexandria, VA 22311

DISTRIBUTION LIST

Dr Gordon C Oehler
Central Intelligence Agency
Washington, DC 20505

Oak Ridge Operations Office
Procurement and Contracts Division
US Department of Energy
(DOE IA No DE-AI05-90ER30174)
PO Box 2001
Oak Ridge, TN 37831-8757

Dr Peter G Pappas
Chief Scientist
US Army Strategic Defense Command
PO Box 15280
Arlington, VA 22215-0280

Dr Aristedes Patrinos [20]
Director of Atmospheric
& Climate Research
ER-74/GTN
US Department of Energy
Washington, DC 20585

Dr Bruce Pierce
USD(A)/D S
Room 3D136
The Pentagon
Washington, DC 20301-3090

Mr John Rausch [2]
Division Head 06 Department
NAVOPINTCEN
4301 Suitland Road
Washington, DC 20390

Records Resources
The MITRE Corporation
Mailstop W115
7525 Colshire Drive
McLean, VA 22102

Dr Oscar S Rothaus
Math Department
Cornell University
Ithaca, NY 14853

Dr Fred E Saalfeld
Director
Office of Naval Research
800 North Quincy Street
Arlington, VA 22217-5000

Dr John Schuster
Technical Director of Submarine
and SSBN Security Program
Department of the Navy OP-02T
The Pentagon Room 4D534
Washington, DC 20350-2000

Dr Barbara Seiders
Chief of Research
Office of Chief Science Advisor
Arms Control & Disarmament Agency
320 21st Street NW
Washington, DC 20451

Dr Philip A Selwyn [2]
Director
Office of Naval Technology
Room 907
800 North Quincy Street
Arlington, VA 22217-5000

DISTRIBUTION LIST

Superintendent
CODE 1424
Attn Documents Librarian
Naval Postgraduate School
Monterey, CA 93943

Dr George W Ullrich [3]
Deputy Director
Defense Nuclear Agency
6801 Telegraph Road
Alexandria, VA 22310

Ms Michelle Van Cleave
Asst Dir/National Security Affairs
Office/Science and Technology Policy
New Executive Office Building
17th and Pennsylvania Avenue
Washington, DC 20506

Mr Richard Vitali
Director of Corporate Laboratory
US Army Laboratory Command
2800 Powder Mill Road
Adelphi, MD 20783-1145

Dr Edward C Whitman
Dep Assistant Secretary of the Navy
C3I Electronic Warfare & Space
Department of the Navy
The Pentagon 4D745
Washington, DC 20350-5000

Mr Donald J. Yockey
U/Secretary of Defense
For Acquisition
The Pentagon Room 3E933
Washington, DC 20301-3000

Dr Linda Zall
Central Intelligence Agency
Washington, DC 20505

Mr Charles A Zraket
Trustee
The MITRE Corporation
Mail Stop A130
Burlington Road
Bedford, MA 01730